Preparation and Characterisation of Thermally Stable $(\overline{\mathrm{SeNSeNSe}})_n(\mathrm{AsF_6})_2$ containing the 'Electron-rich aromatic' 6π $(\overline{\mathrm{SeNSeNSe}})^{2+}$ ($n = 1$) and 7π $\overline{\mathrm{SeNSeNSe}}^{\bullet +}$ ($n = 2$)†

Edward G. Awere, Jack Passmore* and Peter S. White*‡
Department of Chemistry, University of New Brunswick, Fredericton, New Brunswick E3B 6E2, Canada

Crystalline thermally stable $(\overline{\mathrm{SeNSeNSe}})_n(\mathrm{AsF_6})_2$ containing the 'electron-rich aromatic' 6π $\overline{\mathrm{SeNSeNSe}}^{2+}$ ($n = 1$) and 7π radical cation $\overline{\mathrm{SeNSeNSe}}^{\bullet +}$ ($n = 2$) were prepared in high yields from reactions of $\mathrm{Se_4N_4}$ with stoichiometric quantities of $\mathrm{Se_4(AsF_6)_2}$ ($n = 1$) or $\mathrm{AsF_5}$ ($n = 1$ or 2) in liquid $\mathrm{SO_2}$ and their X-ray crystal structures determined. The structure of $\overline{\mathrm{SeNSeNSe}}(\mathrm{AsF_6})_2$ consists of discrete planar $\overline{\mathrm{SeNSeNSe}}^{2+}$ cations and $\mathrm{AsF_6}^-$ anions, and that of $(\overline{\mathrm{SeNSeNSe}})_2(\mathrm{AsF_6})_2$ consists of two identical, but crystallographically different, discrete $(\overline{\mathrm{SeNSeNSe}}^{\bullet +})_2$ cations and $\mathrm{AsF_6}^-$ anions. The centrosymmetric $(\overline{\mathrm{SeNSeNSe}}^{\bullet +})_2$ dimer contains two planar $\overline{\mathrm{SeNSeNSe}}^{\bullet +}$ radical cations weakly joined by two long Se ··· Se bonds [2 × 3.123(3), 2 × 3.149(3) Å]. There are significant cation–anion interactions in both salts. The Se–Se [2.334(3) Å] and Se–N bond lengths [average: 1.74(3) (side), 1.69(3) Å (top)] in $\overline{\mathrm{SeNSeNSe}}^{2+}$ are shorter than their corresponding distances in the 7π $\overline{\mathrm{SeNSeNSe}}^{\bullet +}$ [average: Se–Se 2.398(3); Se–N 1.76(2) (side), 1.69(2) (top) Å] consistent with removal of the unpaired electron from the π^* singly occupied molecular orbital of the monocation. Surprisingly only one peak, rather than the expected two, was observed in the ^{77}Se NMR spectrum of $\overline{\mathrm{SeNSeNSe}}(\mathrm{AsF_6})_2$ consistent with fluxional behaviour in solution. The ^{77}Se chemical shift [−70 °C, $\delta(\mathrm{Me_2Se}) = 2434$, $v_{\frac{1}{2}} = 10$ Hz] is the highest so far recorded and is consistent with the dipositive charge and 'electron-rich' 6π aromatic character. The ^{77}Se and ^{14}N NMR [room temperature (r.t.), $\delta(\mathrm{MeNO_2}) = -67.6$, $v_{\frac{1}{2}} = 200$ Hz] and the Raman spectrum in liquid $\mathrm{AsF_3}$ at 10 °C are all consistent with retention of the $\overline{\mathrm{SeNSeNSe}}^{2+}$ ring structure in solution. The ESR spectrum of $\overline{\mathrm{SeNSeNSe}}^{\bullet +}$ in $\mathrm{SO_2}$ solution at r.t. ($g = 2.043$, broad) and the spectrum of powdered $\overline{\mathrm{SeNSeNSe}}^{\bullet +}$ in frozen $\mathrm{SO_2}$ at −160 °C were similar to but not identical with those of $\overline{\mathrm{SeNSNSe}}^{\bullet +}$, $\overline{\mathrm{SeNSNS}}^{\bullet +}$ and $\overline{\mathrm{SNSNS}}^{\bullet +}$ indicative of a planar 7π ring system.

Numerous binary sulfur–nitrogen species have been prepared and structurally characterised including $\mathrm{SN^+}$, $\mathrm{SNS^+}$, $(\overline{\mathrm{SNSNS}})_2\mathrm{N^+}$, $\overline{\mathrm{SNSNS}}^{\bullet +}$, $(\overline{\mathrm{SNSNS}}^{\bullet +})_2$, $\mathrm{S_4N_3}^+$, $\mathrm{S_4N_4}^{2+}$, $\mathrm{S_4N_5}^+$, $\mathrm{S_5N_5}^+$, $\mathrm{S_2N_2}$, $\mathrm{S_4N_2}$, $\mathrm{S_4N_4}$, $(\mathrm{SN})_x$, $\mathrm{S_3N^-}$, $\mathrm{S_4N^-}$, $\mathrm{S_3N_3}^-$ and $\mathrm{S_4N_5}^-$.[1] These species are interesting because they exhibit diverse structural, physical and electronic properties. Analogous selenium–nitrogen compounds are restricted to $\mathrm{Se_4N_4}$ which is even more thermodynamically and kinetically unstable than $\mathrm{S_4N_4}$ ($\Delta H_f = 460 \pm 8$ for $\mathrm{S_4N_4}$,[2] 682 ± 13 kJ mol^{-1} for $\mathrm{Se_4N_4}$[3]). The chemistry of $\mathrm{Se_4N_4}$ is understandably limited, although there is a growing interest in its reactions. More recently, the preparation of the thermally stable $\mathrm{Se_4N_2}$ has been reported,[4a] but others have produced evidence consistent with this material in fact having the formulation $\mathrm{Se_3N_2Cl_2}$.[4b]

All sulfur–nitrogen cations as salts of very non-basic anions (*e.g.* $\mathrm{AsF_6}^-$) are thermally stable, except $\mathrm{S_4N_5}^+$, in contrast to their neutral and anionic analogues which typically explode or detonate when pure. In addition, the related (N is isoelectronic to $\mathrm{S^+}$) sulfur homopolyatomic cations are more difficult to prepare than their selenium analogues.[5] Therefore, we anticipated that selenium–nitrogen cations would be readily prepared, and that they would be stable. We envisaged that product identification and characterisation would be aided by *in situ* ^{77}Se NMR spectroscopy.

Our earlier attempts to prepare Se–N cations from the reactions of alkali-metal azides with $\mathrm{Se}_n(\mathrm{AsF_6})_n$ ($n = 8$ or 10) were unsuccessful.[6] The ESR spectrum of a frozen solution of powdered $\overline{\mathrm{SeNSNSe}}(\mathrm{AsF_6})_2$ in $\mathrm{SO_2}$ or $\mathrm{D_2SO_4}$ at −196 °C was assigned to $\overline{\mathrm{SeNSNSe}}^{\bullet +}$, a trace of $\overline{\mathrm{SNSNS}}^{\bullet +}$ as well as $\overline{\mathrm{SeNSeNSe}}^{\bullet +}$.[7] These results suggested that $\overline{\mathrm{SeNSNSe}}^{2+}$ was reduced to $\overline{\mathrm{SeNSNSe}}^{\bullet +}$ which then generated $\overline{\mathrm{SNSNS}}^{\bullet +}$ and $\overline{\mathrm{SeNSeNSe}}^{\bullet +}$. Although such a rearrangement was very unusual, it was not totally unprecedented since other unexpected rearrangements have been reported in sulfur–nitrogen chemistry {*e.g.* $2\mathrm{R}\overline{\mathrm{CNSNS}}^{\bullet} \longrightarrow 2\mathrm{R}\overline{\mathrm{CNSSN}}^{\bullet}$ [R = $\mathrm{CF_3}$, Me, I, 2,5-$\mathrm{Me_2C_6H_3}$, Ph, *p*-$\mathrm{O_2NC_6H_4}$, 3,5-$(\mathrm{O_2N})_2\mathrm{C_6H_3}$ or $\mathrm{Bu^t}$][8] and examples cited in ref. 1*b*}. Therefore, the objectives of this work were to prepare binary selenium–nitrogen cations including $\overline{\mathrm{SeNSeNSe}}^{\bullet +}$ and to clarify the ESR results. A preliminary account of this work has been published.[9]

Experimental

General Procedures and Reagents.—Apparatus, chemicals, general techniques and spectrometers used were as described in refs. 10 and 11, unless specified. Raman, IR, mass, ESR, ^{14}N and ^{77}Se NMR samples were prepared and spectra recorded as described in ref. 10; NMR acquisition parameters were as

---

† *Supplementary data available* (No. SUP 56904, 5 pp.): IR and FT-Raman spectra and mass spectral data for $\mathrm{Se_4N_4}$. See Instructions for Authors, *J. Chem. Soc., Dalton Trans.*, 1993, Issue 1, pp. xxiii–xxviii.

‡ *Present address:* Department of Chemistry, The University of North Carolina at Chapel Hill, Chapel Hill, NC 27599-3290, USA.

Non-S.I. unit employed: G = 10^{-4} T.

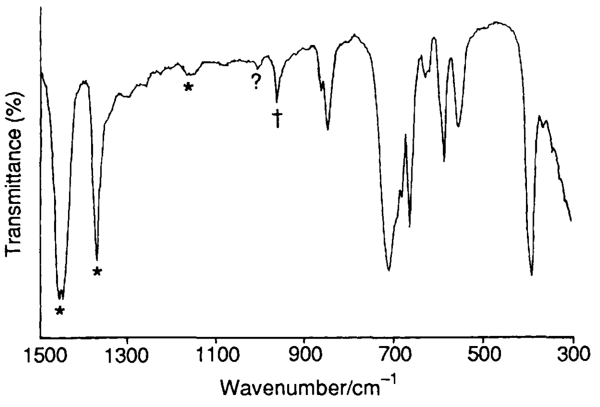

Fig. 1 Infrared spectrum of $(\overline{\mathrm{SeNSeNSe}})_2(\mathrm{AsF}_6)_2$. Nujol peaks indicated by asterisks, peak due to $(\overline{\mathrm{SeNSNSe}})_2(\mathrm{AsF}_6)_2$ indicated by a dagger

previously reported.[10,11] Chemical shifts were externally referenced at room temperature (r.t.) to neat $MeNO_2$ (^{14}N) or neat Me_2Se (^{77}Se) with the high-frequency direction positive. The FT-Raman spectra were recorded at r.t. in a melting-point tube using the FT-Raman accessory FRA106 (Bruker) attached to the FTIR spectrometer IFS66 (Bruker). The 180° arrangement (backscattering mode) was used for data collection [resolution 4 cm^{-1}, 32 scans, laser power: 20 mW (Nd YAG laser)]. Chemical analyses were performed by Beller Mikroanalytisches Laboratorium, Göttingen, Germany.

Sulfur (Fisher Scientific) and selenium (BDH, 99%; Johnson Matthey, 1–3 mm, amorphous, 99.999%, ground to a powder) were vacuum dried. Carbon tetrachloride (Fisher Scientific) was refluxed over P_4O_{10} and distilled onto 3 Å molecular sieves, NH_3 (Canada Liquid Air) was dried over sodium only prior to use, and F_3CCCCF_3 (PCR Research Chemicals) was used without further purification. The compound $SeBr_4$ was prepared from selenium (99 or 99.999%) and an excess of Br_2 in carbon disulfide,[12] $SNAsF_6$[13] and $Se_4(AsF_6)_2$[5] were prepared according to our published methods and $NOAsF_6$[14] was prepared by the reaction of NO with F_2 to give ONF which was treated with AsF_5.

Preparation and Purification of Se_4N_4.—The compound Se_4N_4 was prepared by a modification of the method of Jander and Doetsch.[15] Thus $SeBr_4$ (12.70 g, 31.87 mmol) was loaded into a flame-dried Parr bomb (volume = 70 cm^3) inside a dry-box. The Parr bomb was slowly evacuated for a short period to remove the nitrogen ($SeBr_4$ decomposes[16] to $SeBr_2$ and Br_2 on prolonged evacuation) and an excess of dry ammonia (1.96 g, 115 mmol) was slowly condensed onto the $SeBr_4$ at −196 °C. The reaction mixture was allowed to warm to r.t. and then heated at 60–70 °C for *ca.* 4–5 h in an ultrasonic bath with periodic agitation. After 18 h the Parr bomb was placed in a bath at −50 °C and the valve was slightly opened to allow unreacted ammonia to evaporate into a fumehood. The crude brown product was partially dissolved in distilled water, transferred to a plastic beaker and filtered under suction with a medium filter paper, and then washed with several aliquots of 10% (w/v) aqueous KCN solution until an orange material, Se_4N_4, was obtained (**CAUTION**: KCN is very toxic; the washings were stored in a stoppered bottle and disposed of as described in ref. 17). The purified Se_4N_4 handled in plastic apparatus where ever possible (**CAUTION**: must be kept moist at all times as it is potentially explosive in the dry state) was washed several times with distilled water and dried by washing with several aliquots of anhydrous ethanol and dry CCl_4 under suction, whereas in ref. 15 a desiccant was used as a drying agent. Our modification allows the purified Se_4N_4 to be used immediately or stored in plastic containers under dry CCl_4 at −10 °C and thereby decrease the chances of an explosion. The mass of Se_4N_4 was not obtained because of the danger of an explosion of large amounts of the dry compound. The Se_4N_4 was characterised by its IR spectrum obtained as a Nujol mull (**CAUTION**: two drops of Nujol were added to Se_4N_4 prior to careful grinding). The spectrum [840vw, 785 (sh), 770s, 615w, 570vs, 520 (sh), 480vw, 420vs, 410 (sh), 310m, 295m and 260m cm^{-1}, deposited as SUP 56904] was similar to but not identical with that reported.[18] The IR spectrum obtained after 4 months of storage was identical to that of a freshly prepared sample indicating that hydrolysis or decomposition did not occur within this period. The mass spectrum was obtained using a Teflon ampoule at 70 eV (*ca.* 1.12 × 10^{-17} J) by the direct-inlet method by heating from 40 to 150 °C at a rate of 10 °C min^{-1}. Peaks similar to those reported[19] were obtained but those attributable to $Se_4N_4^+$ and its fragments and Se_x^+ (x = 3–6) were low in intensity. In addition, Se_2^+ rather than Se_2N^+ was the most abundant species [this work (ref. 19): Se_2^+, m/z = 80, 100 (97); Se_2N^+, m/z = 174, 10.3 (100%)]. Full details are included in SUP 56904.

The thermal stability of Se_4N_4 depends on the amount of sulfur present in the selenium used as the starting material for the preparation of $SeBr_4$. Material prepared from $SeBr_4$ using 99.999% selenium exploded more readily than that obtained using 99% selenium. Except where stated, reactions were carried out with the latter sample of Se_4N_4. **CAUTION**: Se_4N_4 is temperature, friction and pressure sensitive. Cooling of the solid compound with liquid nitrogen must be avoided. All the precautions outlined in refs. 15 and 20 were strictly observed and, in addition, thick leather gloves, safety goggles, a face shield and a rubber apron were worn, and experiments conducted behind a safety shield, or explosion-proof glass of a fumehood.

The compound Se_4N_4 was transferred by carefully pipetting a suspension of it in dry CCl_4 into the appropriate reaction vessel with a polyethylene dropper. Some of the supernatant CCl_4 was pipetted out after the solid had settled and the remaining solvent was removed under dynamic vacuum. Fine Se_4N_4 particles adhering to the glass and valve were carefully removed using a Q-tip soaked with dry CCl_4. The mass of Se_4N_4 was obtained first; the required amounts of the other reagents were then deduced on the basis of the stoichiometry of the reaction. The reagents $Se_4(AsF_6)_2$ and $NOAsF_6$ were weighed into a well dried glass tube in a dry-box, sealed with Teflon tape and quickly (< 1 min) transferred onto Se_4N_4 inside a glove bag under dry nitrogen. Volatile materials (SO_2 and AsF_5) were condensed onto Se_4N_4 at −78 °C.

Preparation of $(\overline{\mathrm{SeNSeNSe}})_2(\mathrm{AsF}_6)_2$.—*Reaction of* $Se_4(AsF_6)_2$ *with* Se_4N_4 (1:1 *ratio*). Sulfur dioxide (7.05 g) was condensed onto a mixture of Se_4N_4 (0.60 g, 1.60 mmol) and $Se_4(AsF_6)_2$ (1.06 g, 1.53 mmol) in a one-bulb vessel producing a red-brown solution over a dark brown solid after stirring for 6 h (in order to prevent an Se_4N_4 explosion, the mixture was stirred after a reaction time of *ca.* 2 h when almost all the Se_4N_4 had reacted). After removal of the solvent the resulting brown solid (1.63 g) was finely ground and placed on the glass frit of an extraction vessel joined to a two-bulb vessel. Continuous refluxing with SO_2 (5.2 g) for 3 d produced a red-brown solution over a crystalline black extracted solid and a black insoluble powder (0.317 g Se, mass spectrum) which remained on the frit. The solution was filtered into the second bulb and some solvent (*ca.* 1 cm^3) was recondensed back onto the crystalline solid for purification leading to black crystals [1.08 g, 70% recovered yield based on $Se_4(AsF_6)_2$ used and equation (1) below] and a red-brown solid [0.22 g, $(\overline{\mathrm{SeNSeNSe}})_2(\mathrm{AsF}_6)_2$ containing small amounts of $(\overline{\mathrm{SeNSNSe}})_2(\mathrm{AsF}_6)_2$, IR spectrum] as the more soluble fraction {Found for black crystals [Calc. for $(\overline{\mathrm{SeNSeNSe}})_2(\mathrm{AsF}_6)_2$]: As, 16.35 (16.50); F, 24.80 (25.10); N, 6.05 (6.15); Se, 51.75 (52.20)%}. The IR spectrum of $(\overline{\mathrm{SeNSeNSe}})_2(\mathrm{AsF}_6)_2$ in Nujol is shown in Fig. 1: 1002vw (?),

Table 1 The g and hyperfine tensors for SeNSeNSe$^{\bullet +}$, SeNSNSe$^{\bullet +}$ and SNSNS$^{\bullet +}$ radicals

	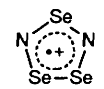		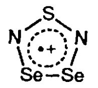		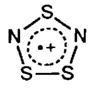
	This work	Ref. 7[a]	This work	Ref. 7	Ref. 7
g_{xx}	*b*	1.9930	*b*	1.9941	2.0020
$a_{xx}(2^{14}N)$/G	9 ± 0.2	7.44	7.25 ± 0.2	6.92	9.34
$a_{xx}(^{77}Se)$/G	*b*	180	*b*	180	
g_{yy}	2.011 ± 0.001	2.0108	2.011 ± 0.001	2.0108	2.0082
$a_{yy}(2^{14}N)$/G	*b*	≈0	*b*	≈0	≈0
$a_{yy}(^{77}Se)$/G	*b*	≈70	*b*	≈70	
g_{zz}	2.123 ± 0.001	2.1379	2.136 ± 0.001	2.1355	2.0258
$a_{zz}(^{77}Se)$/G	43 ± 0.2	43	43 ± 0.2	45	
g_{iso}(22 °C)	2.043 ± 0.001	2.0464	2.046 ± 0.001	2.0464	2.0115

[a] These values were derived from an ESR spectrum of SeNSNSe(AsF$_6$)$_2$ in frozen SO$_2$ under non-rigorously anhydrous conditions at −196 °C. Some of the peaks which we now know arose from SeNSNSe$^{\bullet +}$ appeared as doublets and were erroneously assigned to SeNSNSe$^{\bullet +}$ and SeNSeNSe$^{\bullet +}$. The splitting is likely due to solid-state effects. [b] Value not easily measurable directly from the spectrum.

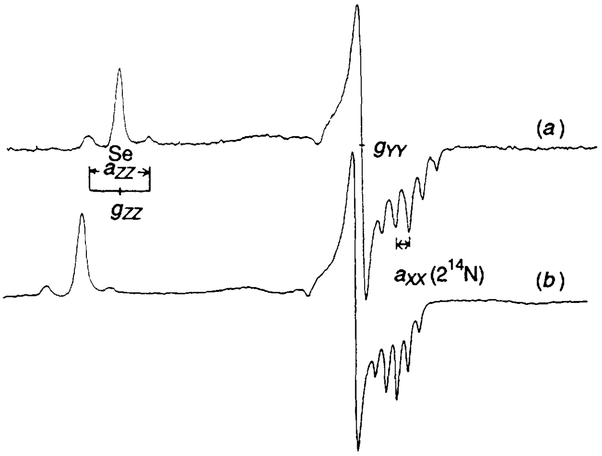

Fig. 2 ESR spectrum of powdered SeNSeNSe$^{\bullet +}$ (*a*) and SeNSNSe$^{\bullet +}$ (*b*) in frozen SO$_2$ at −160 °C under anhydrous conditions

966m (SeNSNSe$^{\bullet +}$), 867w, 848m, 713vs [ν_3(AsF$_6^-$)], 694 (sh), 868 (sh) [ν_1(AsF$_6^-$)], 668m*, 633w, 622vw (SeNSNSe$^{\bullet +}$), 596 (sh), 587m, 555m*, 395s [ν_4(AsF$_6^-$)], 370 (sh) [ν_5(AsF$_6^-$)] and 353vw cm^{-1}; asterisks indicate overlapping with a weak SeNSNSe$^{\bullet +}$ impurity band. A band of moderate intensity at 966 cm^{-1} is attributable to (SeNSNSe)$_2$(AsF$_6$)$_2$ [10] which arises from the sulfur impurity in the Se$_4$N$_4$. The identity of (SeNSeNSe)$_2$(AsF$_6$)$_2$ was confirmed by single-crystal X-ray analysis (see below).

Reaction of Se$_4$N$_4$ *with* AsF$_5$ *according to equation* (2). Arsenic pentafluoride (0.25 g, 1.45 mmol) was condensed onto Se$_4$N$_4$ (0.28 g, 0.75 mmol) in SO$_2$ (2.6 g) in a two-bulb vessel. The mixture was stirred for 6 h producing a red-brown solution over a brown precipitate. The volatile materials including N$_2$ (0.013 g) were removed giving a brown solid [0.494 g, *ca.* 100% yield, (SeNSeNSe)$_2$(AsF$_6$)$_2$ and a trace of (SeNSNSe)$_2$(AsF$_6$)$_2$ [10] (IR spectrum)]. It was critical to use the exact amount of AsF$_5$ required by equation (2) since further oxidation of the product occurs with excess of AsF$_5$ [see equation (4)].

The ESR sample of (SeNSeNSe)$_2$(AsF$_6$)$_2$ in SO$_2$ solution (*ca.* 5.3 × 10^{-4} mol dm^{-3}) was prepared in a quartz ESR tube (outside diameter 3 mm) as described for (SeNSNSe)$_2$(AsF$_6$)$_2$.[10] The ESR spectrum of powdered (SeNSeNSe)$_2$(AsF$_6$)$_2$ in frozen SO$_2$ solution (−160 °C) is compared with that of (SeNSNSe)$_2$(AsF$_6$)$_2$ obtained under the same conditions in Fig. 2 and some ESR parameters are listed in Table 1.

Preparation and Characterisation of SeNSeNSe(AsF$_6$)$_2$.—*Oxidation of* Se$_4$N$_4$ *by* AsF$_5$ *according to equation* (3).—An excess of AsF$_5$ (1.58 g, 9.23 mmol) [relative to the amount required by equation (3)] was condensed onto Se$_4$N$_4$ (0.48 g, 1.3 mmol) in SO$_2$ (4.4 g) in a two-bulb vessel producing a yellow-brown solution over yellow crystals on warming slowly and unstirred from −78 °C to r.t. after 2 h. The solution was filtered into the empty bulb and the yellow crystals were washed twice with the solvent (*ca.* 1 cm^3). Volatile materials and evolved N$_2$ (0.022 g) were removed giving purer highly crystalline light yellow materials [0.73 g, 66% recovered yield based on Se$_4$N$_4$ used and equation (3)] from the less-soluble product and a brownish yellow solid (0.62 g) from the more soluble fraction {Found [Calc. for SeNSeNSe(AsF$_6$)$_2$]: As, 23.15 (23.30); F, 35.30 (35.45); N, 4.60 (4.35); Se, 36.45 (36.85)%}. Single crystals suitable for X-ray structural analysis, IR and Raman (solid) spectra were all obtained from fragments of one large crystal. The identity of SeNSeNSe(AsF$_6$)$_2$ was confirmed by single-crystal X-ray analysis (see below). The IR spectrum of SeNSeNSe(AsF$_6$)$_2$ in Nujol obtained from a fragment of the large crystal was essentially identical to that prepared from purer Se$_4$N$_4$ (from 99.999% Se, see below), except for the presence of a weak band at 976 cm^{-1} attributable to SeNSNSe(AsF$_6$)$_2$. The Raman spectrum of crystalline SeNSeNSe(AsF$_6$)$_2$ at −196 °C [compound decomposed in the laser beam (5145 Å) at r.t.] is shown in Fig. 3 and the Raman spectrum in liquid AsF$_3$ at 10 °C is included in Fig. 4. The frequencies are listed in Table 2, which also includes FT-Raman data. The ^{77}Se NMR spectrum (−70 °C) of SeNSeNSe(AsF$_6$)$_2$ (0.54 g) from the less-soluble fraction in SO$_2$ (2.88 g)–AsF$_5$ (1.79 g) showed resonances at δ 2433.9 ($\nu_{\frac{1}{2}}$ = 9.2), 2411.9 ($\nu_{\frac{1}{2}}$ = 112 Hz, SeNSNSe^{2+})† and 2015.6 ($\nu_{\frac{1}{2}}$ = 10.4 Hz) in the integration ratio of 83 : 1 : 11. We assign the peak at δ 2433.9 to SeNSeNSe^{2+} but that at δ 2015.6 has not been assigned with certainty. The attempts to locate the expected second resonance (apical selenium) for SeNSeNSe^{2+} with an integration ratio of one-half that at δ 2434 over the chemical shift range of δ −308 to 3543 were unsuccessful. The ^{14}N NMR spectrum (r.t.) of SeNSeNSe(AsF$_6$)$_2$ in SO$_2$ showed a broad peak at δ −67.6

---

† We have prepared and characterised SeNSNSe(AsF$_6$)$_2$ (see ref. 10) with δ(^{77}Se) 2412 ($\nu_{\frac{1}{2}}$ = 10.2 Hz) and therefore deduce that the peak at δ 2411.9 is due to SeNSNSe^{2+} which arises from sulfur impurity in the Se$_4$N$_4$.

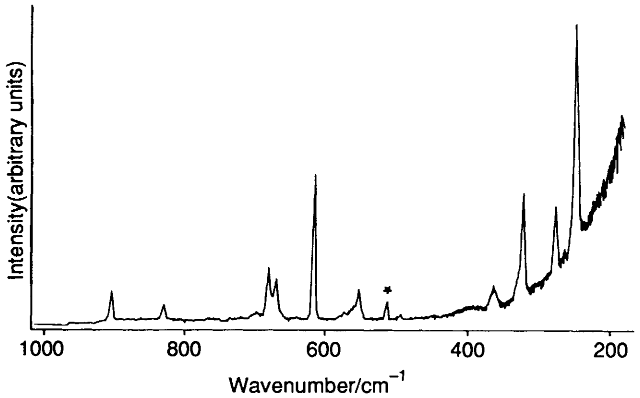

Fig. 3 Raman spectrum of $\mathrm{SeNSeNSe(AsF_6)_2}$ at −196 °C. Peak due to glass indicated by asterisks. Scan range 150–1500 cm^{-1}; power 240 mW; slit 4 cm^{-1}; period 0.5 s; photon counting 1 × 10^5 counts s^{-1}; scan speed 2.5 cm min^{-1}

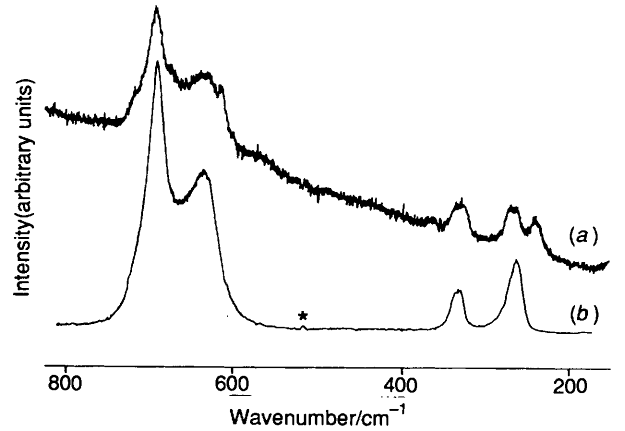

Fig. 4 Raman spectrum of $\mathrm{SeNSeNSe(AsF_6)_2}$ in liquid AsF_3 at 10 °C (a) and liquid AsF_3 (b). Peak due to glass indicated by asterisk

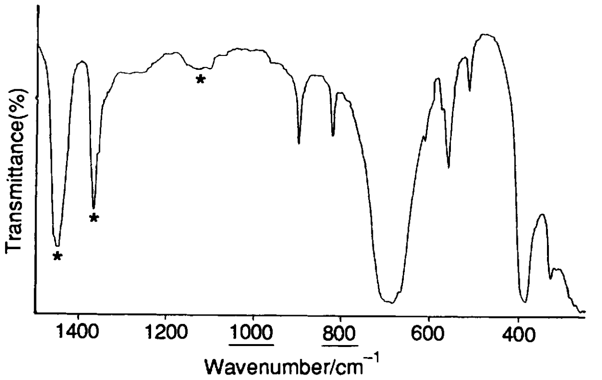

Fig. 5 Infrared spectrum of $\mathrm{SeNSeNSe(AsF_6)_2}$. Nujol peaks indicated by asterisks

($\nu_{\frac{1}{2}}$ = 200 Hz) and its mass spectrum showed intense peaks attributable to the fragmentation of AsF_5 (*i.e.* AsF_4^+ to As^+) and weak peaks containing Se–N fragments.

The IR spectrum of the more soluble product showed mainly the presence of $\mathrm{SeNSeNSe(AsF_6)_2}$ and small amounts of $\mathrm{SeNSNSe(AsF_6)_2}$[10] whilst the ^{77}Se NMR spectrum (−70 °C) showed two resonances at δ 2435.3 ($\nu_{\frac{1}{2}}$ = 9.5, $\mathrm{SeNSeNSe^{2+}}$) and 2016.7 ($\nu_{\frac{1}{2}}$ = 10.5 Hz, unassigned) in the integration ratio of 8 : 1.

Table 2 Vibrational data (corrected) for $\mathrm{SeNSeNSe(AsF_6)_2}$ and tentative assignments[a]

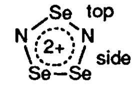

IR (Nujol) (Fig. 5)	Raman: Solid[b] (Fig. 3) at −196 °C, 5145 Å	Raman: In AsF_3(l)[c] (Fig. 4)	Assignment
908m	906 (12)		ν_{sym}(SeN) top
830m	836 (10)		ν_{asym}(SeN) top
		720vw *	?
698vs (br)	698 (< 12)		$\nu_3(AsF_6^-)$[d]
	684 (22)	682vw *	$\nu_1(AsF_6^-)$[d]
670 (sh)	672 (20)		
619m	619 (49)	618vw *	ν_{sym}(SeN) side and top[e]
583 (sh)	576 (< 12)		$\nu_2(AsF_6^-)$[d]
567m	558 (19)		
520w			ν_{asym}(SeN) side
	495 (< 12)		?
393s	400 (< 12)		$\nu_4(AsF_6^-)$[d]
	367 (18)	370vw	$\nu_5(AsF_6^-)$[d]
339s[f]	325 (54)	332m	ν_{sym}(Se–Se)[e]
308 (sh)			?
	276 (30)	270m[g]	Bend (bottom)[h]
	249 (100)	247m	Bend (top)[h]

v = Very, s = strong, m = medium, w = weak, sh = shoulder, br = broad; asterisks indicate overlapping with strong and broad AsF_3 bands.

[a] Based on a full normal coordinate analysis which will be reported elsewhere.[21] The symmetric and asymmetric stretching vibrations transform as A_1 and B_2, respectively. [b] Relative areas are given in parentheses. FT-Raman spectrum at room temperature, 910 (14), 831 (5), 684 (100), 622 (41), 562 (36), 518 (5), 370 (18), 327 (50), 281 (23), 250 (41). Actual spectrum is included in SUP 56904. [c] Relative areas could not be obtained because some of the peaks overlapped with AsF_3 bands (see Fig. 4); AsF_3 peaks are not included. [d] By comparison with AsF_6^- salts, ref. 22. [e] Mixed with bend. [f] This peak is weak in Fig. 5 due to KBr cut-off but it is strong and well resolved using CsI plates. [g] Peak overlaps with a moderately intense AsF_3 band. [h] Mixed with Se–N vibration.

In other similar reactions carried out *in situ* in 10 mm NMR tubes, with and without Br_2, similar results were obtained except that in some, but not all, the reactions additional weak resonances in the ^{77}Se NMR spectrum were observed at δ 2016, 1750 and 1733.

The oxidation of Se_4N_4 (prepared from 99.999% Se) with AsF_5 according to equation (3) was carried out as described above for the less-pure Se_4N_4. The IR spectrum of purified $\mathrm{SeNSeNSe(AsF_6)_2}$ is shown in Fig. 5 in which detectable amounts of $\mathrm{SeNSNSe(AsF_6)_2}$ were not observed. The vibrational data for $\mathrm{SeNSeNSe(AsF_6)_2}$ are given in Table 2. A sample prepared *in situ* in a 10 mm thick-walled NMR tube from Se_4N_4 [prepared from 99.999% Se, 0.25 g, 0.67 mmol; AsF_5 (0.63 g, 3.70 mmol) in SO_2 (3.48 g)] gave a clear yellow-brown solution after 2 h. The ^{77}Se NMR spectrum (−70 °C) contained three resonances [δ 2434.1 ($\nu_{\frac{1}{2}}$ = 10.2), $\mathrm{SeNSeNSe^{2+}}$), 2412.1 ($\nu_{\frac{1}{2}}$ = 10.5, $\mathrm{SeNSNSe^{2+}}$),[10] and 2015.8 ($\nu_{\frac{1}{2}}$ = 13.1 Hz, unassigned)] in the integration ratio of 28 : 1 : 5.

Oxidation of $\mathrm{(SeNSeNSe)_2(AsF_6)_2}$ *by* AsF_5 *according to equation* (4). A slight excess of AsF_5 (0.42 g, 2.47 mmol) relative to the amount required by equation (4) was condensed at −196 °C onto $\mathrm{(SeNSeNSe)_2(AsF_6)_2}$ [0.319 g, 0.35 mmol; prepared according to equation (1)] in SO_2 (2.88 g) in a 10 mm thick-walled NMR tube. After 1 h at r.t. a transparent yellow solution was formed over a yellow crystalline solid which dissolved on cooling to −70 °C. The ^{77}Se NMR spectrum (−70 °C) showed peaks at δ 2434.0 ($\nu_{\frac{1}{2}}$ = 10.1, $SeNSeNSe^{2+}$), 2411.9 ($\nu_{\frac{1}{2}}$ = 12.4, $SeNSNSe^{2+}$) and 2015.8 ($\nu_{\frac{1}{2}}$ = 13.1 Hz, unassigned) in the integration ratio of 8:4.7:1. The IR spectrum of the resulting light yellow solid (0.463 g) showed mainly the presence of $SeNSeNSe(AsF_6)_2$ with small amounts of $SeNSNSe(AsF_6)_2$.

The oxidation of $(SeNSeNSe)_2(AsF_6)_2$ [prepared according to equation (2)] led also to $SeNSeNSe(AsF_6)_2$ with small amounts of $SeNSNSe(AsF_6)_2$. This was confirmed by IR and ^{77}Se NMR spectroscopy [−70 °C: δ 2434.2 ($\nu_{\frac{1}{2}}$ = 12.5, $SeNSeNSe^{2+}$) and 2412.2 ($\nu_{\frac{1}{2}}$ = 12.0 Hz, $SeNSNSe^{2+}$); integration ratio: 3.6:1].

Some Physical Properties of $(SeNSeNSe)_n(AsF_6)_2$ (*n* = 1 or 2).—Crystals of $SeNSeNSe(AsF_6)_2$ are yellow and transparent colourless in reflected and transmitted light, respectively. The compound decomposes at 176 °C to give a brown solid (m.p. 294 °C, black liquid) without exploding. It does not detonate on grinding, cooling to −196 °C or on manipulation with a nickel spatula which shows that the compound is thermally stable, in contrast to Se_4N_4. A solution of $SeNSeNSe(AsF_6)_2$ in liquid AsF_3 heated at 55 °C for 1 h did not lose N_2 while a solid sample heated at 140 °C for 4 d *in vacuo* [*ca.* 10^{-3} Torr (*ca.* 0.13 Pa)] in a sealed tube still contained some of the original compound (IR spectrum). The compound $SeNSeNSe(AsF_6)_2$ is sparingly soluble in liquid SO_2 (*ca* 9% w/w), but dissolves readily in SO_2 (2.88 g)–AsF_5 (1.79 g) at *ca.* −40 °C, increasing in solubility as the temperature is lowered and is moderately soluble in AsF_3 (*ca.* 20% w/w). It is sensitive to traces of moist air and rapidly acquires a brown coating. The ^{77}Se NMR spectrum of a fresh solution of $SeNSeNSe(AsF_6)_2$ prepared *in situ* with an excess of AsF_5 showed a weak resonance at 10 °C (δ 2438.1, $\nu_{\frac{1}{2}}$ = 26.9 Hz) [*cf.* at −70 °C (δ 2433.1, $\nu_{\frac{1}{2}}$ = 15.0 Hz)]. However, if the compound is manipulated inside a dry-box and then redissolved in SO_2 this peak is observed only at low temperature (*e.g.* at −70 °C). The IR spectrum does not change on prolonged grinding or on subjection to dynamic vacuum for a long period which shows that, in contrast to $SNSNS^{2+}$ in $SNSNS(AsF_6)_2$,[23] the $SeNSeNSe^{2+}$ cation does not abstract a fluoride ion from AsF_6^- to form $FSeNSeNSe^+$. A solution of $SeNSeNSe(AsF_6)_2$ in SO_2 was treated with excess of CCl_3F for 18 h and the IR spectrum of the resulting solid was identical to that of the original compound which implied that the $SeNSeNSe^{2+}$ cation did not abstract a chloride ion, in contrast to $SeNSNS^{2+}$ (ref. 24) and $SeNSNSe^{2+}$.[10]

Crystals of $(SeNSeNSe)_2(AsF_6)_2$ are greenish black in room light but black in reflected and transmitted light when viewed under the microscope, and reddish brown in the powdered form. The compound does not explode on heating (m.p. 178–180 °C, black liquid), cooling to −196 °C or on grinding or handling with a nickel spatula. It is sparingly soluble in liquid SO_2.

Samples of $(SeNSeNSe)_n(AsF_6)_2$ (*n* = 1 or 2) were sealed in separate well dried glass tubes under dry N_2 and stored at −20 °C for more than 1 y without decomposition or loss of crystallinity, and their IR spectra were identical to those of the freshly prepared crystalline compounds.

Reaction of $SeNSeNSe(AsF_6)_2$ *with* F_3CCCCF_3 *or* $SNAsF_6$ (1:1 *ratio*).—The compounds $SeNSeNSe(AsF_6)_2$ (0.34 g, 0.52 mmol) and F_3CCCCF_3 (1.09 g, 6.7 mmol) in SO_2 (3.27 g) in a 10 mm thick-walled NMR tube did not produce any colour change after *ca.* 18 h and contained only the starting materials (^{77}Se NMR spectroscopy). The reaction mixture was heated at 50 °C for 10 d with no observable change (colour and ^{77}Se NMR spectrum). The appearance and IR spectrum of the solid remaining after work-up (0.34 g) indicated that no reaction occurred.

In a similar reaction $SeNSeNSe(AsF_6)_2$ (0.77 g, 1.20 mmol) and $SNAsF_6$ (0.29 g, 1.23 mmol) were mixed in SO_2 (3.25 g) in a 10 mm thick-walled NMR tube at −70 °C with no colour change on reaching r.t. The ^{77}Se NMR spectrum acquired after 15 min showed $SeNSeNSe^{2+}$ and a peak at δ 2015.6 (unidentified species) in the integration ratio of 7.6:1. No reaction occurred at r.t. after 1 week with periodic shaking (no colour change, ^{77}Se and ^{14}N NMR spectroscopy). The solid remaining after work-up (1.04 g) was identical (IR spectrum) to the starting material.

Attempted Preparation of $Se_4N_4(AsF_6)_2$.—*Reaction of* Se_4N_4 *with* AsF_5. Arsenic pentafluoride (0.43 g, 2.53 mmol) and a trace of Br_2 were successively condensed onto Se_4N_4 (0.23 g, 0.62 mmol) in SO_2 (2.92 g) in a two-bulb vessel producing a green solution at r.t., and a red-brown solution over light yellow crystals after *ca.* 10 min. The solution was filtered into the second bulb and the crystals were washed with SO_2 (*ca.* 3 cm^3). The solvent was then slowly condensed into the first bulb which was cooled with dripping cold tap water (*ca.* 10 °C). After 12 h volatile materials were removed giving light yellow crystals [0.215 g, $SeNSeNSe(AsF_6)_2$, IR spectrum] as the less-soluble product and an amorphous opaque red-brown solid (0.45 g) as the more soluble product. IR spectrum in Nujol, CsI plates: 1166 (sh), 1126 (sh), 1106s (br), 907vw*, 857ms (br), 833vw*, 807vw, 775 (sh), 707vs (AsF_6^-), 627vw*, 577vw*, 563w*, 520vw*, 390s (AsF_6^-), 360 (sh) and 337w* cm^{-1} [* attributable to $SeNSeNSe(AsF_6)_2$ impurity]. This red solid is likely not the cause of one of the unidentified resonances in the ^{77}Se NMR spectra observed above as the resulting solids were yellow, *i.e.* seemed to contain no red coloured component.

In similar reactions (mole ratio of Se_4N_4:AsF_5 = 1:3 to 1:4),[25] the attempt to grow crystals of the red-brown product from SO_2 led to the formation of $SeNSeNSe(AsF_6)_2$ (IR spectrum) and the evolution of N_2.

Reaction of Se_4N_4 *with* $NOAsF_6$ (1:2 *ratio*). A solution of $NOAsF_6$ (0.27 g, 1.20 mmol) in SO_2 (3.45 g) was poured onto Se_4N_4 (0.22 g, 0.58 mmol) at r.t. in a two-bulb vessel incorporating two J-Young valves. An intense red-brown solution formed with no solid material, accompanied by effervescence. After 18 h a red-brown solid formed but the colour of the solution did not change. Volatile materials (N_2O, SiF_4 and SO_2, IR spectra) and evolved N_2 (0.01 g) were removed giving a brown solid [0.468 g, $(SeNSeNSe)_2(AsF_6)_2$, IR spectrum].

X-Ray Crystallographic Analysis of $(SeNSeNSe)_n(AsF_6)_2$ (*n* = 1 *or* 2).—Diffraction intensities were measured at 293 K on an Enraf-Nonius CAD-4 diffractometer equipped with graphite-monochromated Mo-Kα radiation (λ = 0.710 73 Å) using the NRCCAD[26] control program. An ω–2θ scan was used and backgrounds were estimated by extending the scan by 25% on either side of the scan limits. The limits of the peak were then ascertained by profile analysis to provide an improved background correction. Unit-cell parameters were obtained by least-squares refinement using the coordinates of 15 (*n* = 2, 2θ range 30–40°) and 25 (*n* = 1, 2θ range 30–35°) reflections, centred using the TRUANG option of NRCCAD, thereby minimising the effects of instrumental and crystal-alignment errors. Lorentz and polarisation factors were applied and absorption corrections were made using the empirical routine of Walker and Stuart.[27]

The structure was solved by direct-methods techniques and

Table 3 Crystallographic data for $\mathrm{(SeNSeNSe)_{\mathit{n}}(AsF_6)_2}$ ($n = 1$ or 2)

	$\mathrm{SeNSeNSe(AsF_6)_2}$	$\mathrm{(SeNSeNSe)_2(AsF_6)_2}$
Formula	$\mathrm{As_2F_{12}N_2Se_3}$	$\mathrm{As_2F_{12}N_4Se_6}$
M	642.49	907.29
Crystal size/mm	0.69 × 0.46 × 0.35	0.30 × 0.30 × 0.20
System	Monoclinic	Triclinic
Space group	$C2$	$P\bar{1}$
a/Å	12.799(2)	8.213(2)
b/Å	8.6837(9)	10.325(2)
c/Å	10.813(1)	10.452(1)
α/°		82.38(1)
β/°	91.467(9)	82.44(1)
γ/°		70.54(1)
U/Å^3	1201.4	824.7
Z (molecules per cell)	4	2
F(000)	1160	406
D_c/Mg m^{-3}	3.55	3.66
μ(Mo-Kα)/mm^{-1}	14.69	8.64
Reflections measured	1125	2876
Unique reflections	1125	2876
Unique reflections, $I_{net} > 2.50\sigma(I_{net})$	935	1860
R^a (observed, all)	0.052, 0.064	0.051, 0.096
R'^b (observed, all)	0.062, 0.065	0.064, 0.076

[a] $\Sigma||F_o| - |F_c||/\Sigma|F_o|$. [b] $[\Sigma w(|F_o| - |F_c|)^2/\Sigma w|F_o|^2]^{\frac{1}{2}}$, where $w = 1/\sigma^2 I$.

Table 4 Fractional atomic parameters with estimated standard deviations (e.s.d.s) in parentheses

	X/a	Y/b	Z/c
$\mathrm{SeNSeNSe(AsF_6)_2}$			
Se(1)	0.292 6(2)	0.763 04	0.357 2(2)
Se(2)	0.288 6(2)	0.760 0(3)	0.141 4(2)
Se(3)	0.358 4(2)	1.065 0(3)	0.247 7(2)
N(1)	0.329(1)	0.951(2)	0.125(2)
N(2)	0.331(1)	0.954(3)	0.372(2)
As(1)	0	0.897 7(4)	1/2
F(11)	−0.068(2)	0.773(3)	0.420(2)
F(12)	0.068(2)	1.036(3)	0.574(2)
F(13)	−0.087(2)	0.919(4)	0.609(2)
As(2)	1/2	0.393 9(4)	0
F(21)	0.420(1)	0.404(3)	−0.125(2)
F(22)	0.575(1)	0.545(2)	−0.063(2)
F(23)	0.423(1)	0.260(2)	0.058(2)
As(3)	0.135 8(1)	0.376 2(3)	0.248 9(2)
F(31)	0.089(2)	0.502(3)	0.362(2)
F(32)	0.189(1)	0.269(2)	0.140(1)
F(33)	0.080(2)	0.502(3)	0.138(2)
F(34)	0.245(1)	0.490(2)	0.248(2)
F(35)	0.191(1)	0.270(2)	0.358(1)
F(36)	0.026(1)	0.284(2)	0.247(2)
$\mathrm{(SeNSeNSe)_2(AsF_6)_2}$			
Se(1)	0.282 4(3)	0.473 2(2)	0.078 8(2)
Se(2)	0.331 0(3)	0.688 4(2)	0.004 6(2)
Se(3)	0.294 4(3)	0.634 7(2)	0.293 9(2)
N(1)	0.270(2)	0.493(2)	0.245(2)
N(2)	0.322(2)	0.739(1)	0.160(1)
Se(4)	0.264 2(3)	0.988 0(2)	0.519 9(2)
Se(5)	0.348 9(3)	1.185 4(2)	0.434 1(2)
Se(6)	0.267 5(3)	1.041 7(2)	0.229 2(2)
N(3)	0.232(2)	0.946(1)	0.372(1)
N(4)	0.328(2)	1.172(1)	0.270(1)
As(1)	0.793 3(2)	0.376 2(2)	0.324 6(2)
F(11)	0.963(2)	0.394(2)	0.228(2)
F(12)	0.664(2)	0.470(1)	0.204(1)
F(13)	0.620(2)	0.353(2)	0.417(1)
F(14)	0.921(2)	0.274(2)	0.437(1)
F(15)	0.760(3)	0.517(2)	0.395(1)
F(16)	0.819(3)	0.230(1)	0.259(2)
As(2)	0.787 5(3)	0.860 7(2)	0.146 6(2)
F(21)	0.925(2)	0.855(2)	0.010(1)
F(22)	0.650(2)	0.872(2)	0.285(1)
F(23)	0.662(2)	0.809(2)	0.075(2)
F(24)	0.916(2)	0.920(3)	0.219(2)
F(25)	0.912(2)	0.711(2)	0.202(2)
F(26)	0.671(2)	1.021(2)	0.093(2)

subsequent difference syntheses. Crystal data are summarised in Table 3. Refinement was by full-matrix least squares with weights based on counter statistics. All atoms were refined with anisotropic thermal parameters. Computations were performed using the NRCVAX suite of crystal structure programs.[28] Scattering factors were taken from ref. 29 and were corrected for anomalous dispersion. The final atomic coordinates are given in Table 4.

Additional material available from the Cambridge Crystallographic Data Centre comprises thermal parameters and remaining bond lengths and angles.

Results and Discussion

Preparation and Characterisation of $\mathrm{(SeNSeNSe)_2(AsF_6)_2}$.—The compound $\mathrm{(SeNSeNSe)_2(AsF_6)_2}$ was prepared from the reaction of $\mathrm{Se_4N_4}$ with stoichiometric quantities of $\mathrm{Se_4(AsF_6)_2}$ or $\mathrm{AsF_5}$ according to equations (1) and (2), respectively. The

$$\mathrm{Se_4N_4 + Se_4(AsF_6)_2 \longrightarrow (SeNSeNSe)_2(AsF_6)_2 + 2Se} \quad (1)$$

$$\mathrm{3Se_4N_4 + 6AsF_5 \longrightarrow 2(SeNSeNSe)_2(AsF_6)_2 + 2N_2 + 2AsF_3} \quad (2)$$

success of reaction (1) was not surprising as it was designed on the basis of the analogous reactions of $\mathrm{S_4N_4}$ with $\mathrm{S_4(AsF_6)_2}$ or with $\mathrm{Se_4(AsF_6)_2}$ which give $\mathrm{(SNSNS)_2(AsF_6)_2}$[11] and $\mathrm{(SeNSNSe)_2(AsF_6)_2}$,[10,30] respectively. However, there is no analogy of reaction (2) in $\mathrm{S_4N_4}$ chemistry (see below). The reaction of $\mathrm{Se_4N_4}$ with $\mathrm{Se_4(AsF_6)_2}$ was complete within *ca.* 18 h (colour changes and the precipitation of a black solid) while reaction (2) proceeded in essentially quantitative yield within *ca.* 1 h. The bulk of the product from the reaction of $\mathrm{Se_4N_4}$ with $\mathrm{Se_4(AsF_6)_2}$ was extracted with refluxing $\mathrm{SO_2}$ and worked up to produce greenish black crystalline purified $\mathrm{(SeNSeNSe)_2(AsF_6)_2}$ (1.08 g, *ca.* 80% isolated yield). The product was identified by chemical analyses, IR and ESR spectroscopy, and confirmed by its X-ray crystal structure (see below). The ESR spectrum of $\mathrm{SeNSeNSe^{\bullet +}}$ in $\mathrm{SO_2}$ at r.t. ($g = 2.043$, broad) and the ESR spectrum of the powder in frozen $\mathrm{SO_2}$ at −160 °C are similar to but not identical with those of the related 7π radical cations[7] $\mathrm{SeNSNSe^{\bullet +}}$ and $\mathrm{SeNSNS^{\bullet +}}$ (see Fig. 2 and Table 1). The powder ESR spectra of these radicals including $\mathrm{SeNSeNSe^{\bullet +}}$ show a close resemblance to that of the 7π cyclic $\mathrm{SNSNS^{\bullet +}}$,[31,32] the spectrum of which has been rigorously assigned. Thus the identity of $\mathrm{SeNSeNSe^{\bullet +}}$ has been established in solution. Our ESR parameters for $\mathrm{SeNSeNSe^{\bullet +}}$ are very different from those previously[7] assigned to this cation. The ESR data obtained from $\mathrm{SeNSNSe(AsF_6)_2}$ in frozen $\mathrm{D_2SO_4}$ or $\mathrm{SO_2}$ agree well for $\mathrm{SeNSNSe^{\bullet +}}$ but not $\mathrm{SeNSeNSe^{\bullet +}}$ (see Fig. 2 and Table 1) showing that the previous assignment[7] of the spectrum to a mixture of $\mathrm{SeNSNSe^{\bullet +}}$ and $\mathrm{SeNSeNSe^{\bullet +}}$ was erroneous. This assignment was not unreasonable because the singly occupied molecular orbital (SOMO) of both radicals has a node through the unique chalcogen atom and therefore might be expected to give rise to similar ESR spectra. The trends in the ESR parameters of the $Se_{3-x}S_xN_2^{\cdot +}$ (x = 0–3) radicals have been rationalised by Preston and Sutcliffe.[33]

The purity of $(SeNSeNSe)_2(AsF_6)_2$ was assessed by its IR spectrum and by the ^{77}Se NMR (−70 °C) and IR spectra of the product given on oxidation by AsF_5. The identity of $(SeNSeNSe)_2(AsF_6)_2$ was also inferred from the ^{77}Se NMR and IR spectra of the oxidised product which showed $SeNSeNSe^{2+}$ and small amounts of $SeNSNSe^{2+}$ and an unknown species [$\delta(^{77}Se)$ 2015.8, $\nu_{\frac{1}{2}} = 13.1$ Hz]. The proportion of the former compound was higher in the sample prepared according to equation (1) than in that prepared according to equation (2) which may be due to an increase in the relative amount of sulfur as selenium is precipitated in the former reaction. We have prepared pure $(SeNSNSe)_2(AsF_6)_2$ by the reduction of purified $SeNSNSe(AsF_6)_2$ with CsN_3 in liquid SO_2.[10] It should therefore be possible to prepare purer $(SeNSeNSe)_2(AsF_6)_2$ in a similar manner, although this was not attempted in this study. The oxidation of Se_4N_4 (prepared from 99.999% Se) with AsF_5 according to equation (2) would also afford purer $(SeNSeNSe)_2(AsF_6)_2$.

Preparation and Characterisation of $SeNSeNSe(AsF_6)_2$.—The compound $SeNSeNSe(AsF_6)_2$ was prepared from the oxidation of Se_4N_4 by AsF_5 according to equation (3). The

$$3Se_4N_4 + 12AsF_5 \longrightarrow 4SeNSeNSe(AsF_6)_2 + 2N_2 + 4AsF_3 \quad (3)$$

reaction was complete within *ca.* 1 h as indicated by the colour changes and the formation of crystalline materials. The product was identified as $SeNSeNSe(AsF_6)_2$ by chemical analyses, IR and Raman spectroscopy with assignments supported by normal coordinate analysis,[21] and confirmed by its X-ray crystal structure. Purification was effected by fractional crystallisation, the less-soluble fraction gave light yellow crystalline $SeNSeNSe(AsF_6)_2$ (*e.g.* 0.73 g, 66% isolated yield), as well as $SeNSNSe(AsF_6)_2$[10] and an unidentified species $\delta(^{77}Se)$ 2015.6, $\nu_{\frac{1}{2}}$ 10.4 Hz, integration ratio $SeNSeNSe^{2+}$: $SeNSNSe^{2+}$: unidentified species = 83 : 1 : 11. The more soluble portion contained a greater concentration of impurities. In *in situ* reactions the ratios of the $SeNSeNSe^{2+}$ to $SeNSNSe^{2+}$ integrated peak heights (^{77}Se NMR) were typically *ca.* 9 : 1. However, a sample prepared from Se_4N_4 (99.999% Se starting material) contained lower amounts of $SeNSNSe^{2+}$ (integration ratio of $SeNSeNSe^{2+}$: $SeNSNSe^{2+}$ = 28 : 1, ^{77}Se NMR spectrum) which was not detectable in the IR spectrum (see Fig. 5). The oxidation of $(SeNSeNSe)_2(AsF_6)_2$ by AsF_5 according to equation (4) also gave $SeNSeNSe(AsF_6)_2$ in essentially quantitative yield.

$$(SeNSeNSe)_2(AsF_6)_2 + 3AsF_5 \longrightarrow 2SeNSeNSe(AsF_6)_2 + AsF_3 \quad (4)$$

The ease with which Se_4N_4 loses N_2 on oxidation by AsF_5 [see equations (2) and (3)] to give $(SeNSeNSe)_n(AsF_6)_2$ (n = 1 or 2) can be contrasted with the behaviour of S_4N_4 which on oxidation by AsF_5 (1 : 3 ratio or excess) gives $S_4N_4(AsF_6)_2$ (70%), $SNAsF_6$ (30%) and a trace amount of $SNSAsF_6$.[10,34] Several attempts to prepare $Se_4N_4(AsF_6)_2$ by oxidation of Se_4N_4 with AsF_5 were unsuccessful and instead gave an unidentified light red-brown compound which readily lost N_2 (pink discharge imparted by Tesla coil) to give $SeNSeNSe(AsF_6)_2$ on redissolving in SO_2. The unidentified compound was formed at a Se_4N_4 : AsF_5 mole ratio of 1 : 3 to 1 : 4, although similar reactions carried out using these ratios gave $SeNSeNSe(AsF_6)_2$ and N_2 showing that the reaction is not easily reproducible.[25] In addition, various attempts to oxidise Se_4N_4 without loss of N_2 (*e.g.* with $NOAsF_6$ or Cl_2 and AsF_5[25]) were unsuccessful (see Experimental section).

As far as we are aware the compounds $(SeNSeNSe)_n(AsF_6)_2$ (n = 1 or 2) are the first examples of the successful preparation, isolation and structural characterisation of compounds containing thermally stable binary Se–N species. Since our preliminary publication[9] the preparation of the thermally stable Se_4N_2 has been reported[4a] but others have provided evidence that 'Se_4N_2' has properties consistent with the formulation $Se_3N_2Cl_2$.[4b] Several selenium(IV) compounds containing the $-N{=}SeX_2$ (X = F or Cl)[35a,b] and $-N{=}Se{=}N-$ moieties[35c] and compounds of the type $Cl_2RSe{-}N{=}SeRCl$ (R = aryl)[35d] are thermally unstable at ambient temperatures. The stability of the binary Se–N cations may therefore be attributed in part to their crystal lattice energies. In addition, the replacement of Se^{II} by a trivalent Se^+ results in the formation of three rather than two bonds which may also be stronger because of the positive charge.

The Nature of the $SeNSeNSe^{2+}$ *Cation in Solution.*—The $SeNSeNSe^{2+}$ cation is expected to give two resonances in the integration ratio of 2 : 1 with satellite peaks due to ^{77}Se–^{77}Se coupling (^{77}Se spin $\frac{1}{2}$, natural abundance 7.50%) in the ^{77}Se NMR spectrum (see **I**). However, the ^{77}Se NMR spectrum (−70 °C) of a solution of $SeNSeNSe(AsF_6)_2$ prepared *in situ* or redissolved in a SO_2–AsF_5 mixture showed a strong peak at δ 2434 with no satellite peaks due to ^{77}Se–^{77}Se coupling. Surprisingly, another resonance with an integration ratio one half of that at δ 2434 was not observed over the chemical shift range of δ −308 to 3543. It is unlikely that the unassigned peak at δ 2016 is due to $SeNSeNSe^{2+}$ since the intensity of the peak was low [integration ratio of δ 2016 (unassigned) to δ 2434 ($SeNSeNSe^{2+}$) was *ca.* 1 : 7] and varied from sample to sample. The peak at δ 2434 is the highest ^{77}Se NMR chemical shift so far recorded and indicates that the Se nuclei are strongly deshielded consistent with the dipositive charge and a delocalised ring 6π system. Similar ^{77}Se NMR chemical shifts were observed for the related cations $SeNSNSe^{2+}$ (δ 2412)[10] and $SeNSNS^{2+}$ (δ 2422).[24] The resonances of these cations are expected to shift to a higher frequency as selenium is replaced by the more electronegative sulfur. The chemical shift trend of $SeNSNSe^{2+}$ and $SeNSNS^{2+}$ is consistent with this rationale, but that of $SeNSeNSe^{2+}$ (δ 2434) is somewhat higher than expected, presumably due to the presence of a rapid process in solution (see below) which averages the value of the chemical shifts of Se_A and Se_B (see **I**).

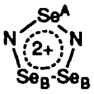

I

The presence of one, rather than the expected two resonances for $SeNSeNSe^{2+}$ in the ^{77}Se NMR spectrum and the absence of satellite peaks due to ^{77}Se–^{77}Se spin coupling suggested that a rapid equilibrium may exist in solution [see equation (5a)]. If

$$SeNSeNSe^{2+} \underset{}{\overset{SO_2}{\rightleftharpoons}} SeNSe^{+} + SeN^{+} \quad (5a)$$

$$cf.\ SNSNS^{2+} \xrightarrow{SO_2} SNS^{+} + SN^{+} \quad (5b)$$

$SeNSeNSe^{2+}$ was in equilibrium with $SeNSe^+$ and SeN^+ then a significant change in the average chemical shift would be expected on changing the temperature. The analogous $SNSNS^{2+}$ in $SNSNS(AsF_6)_2$ completely dissociates in solution [equation (5b)], although the salt is formed by a lattice-enforced symmetry-allowed cycloaddition reaction on formation of the solid.[21,23]

However, the ^{77}Se NMR chemical shift of $SeNSeNSe^{2+}$ at −70 °C (δ 2434) was essentially the same as that at 10 °C (δ 2438) which indicates that if the $SeNSeNSe^{2+}$ cation dissociates in solution then the extent is very small. The ^{14}N NMR spectrum of $SeNSeNSe(AsF_6)_2$ in SO_2 showed one broad peak (δ −67.6, $\nu_{\frac{1}{2}}$ = 200 Hz) consistent with a ring structure, rather than small Se–N containing species such as $SeNSe^+$ or SeN^+ [*cf.* $\delta(^{14}N)$ 202, $\nu_{\frac{1}{2}}$ = 240 Hz for NS^+; δ −91, $\nu_{\frac{1}{2}}$ = 8 Hz for SNS^+][11] both of which would be expected to have relatively sharp peaks. In addition, the Raman spectrum in liquid AsF_3 showed a moderately intense band at 332 cm^{-1} which has been assigned to an Se–Se stretching vibration as well as some of the strong peaks observed in the Raman spectrum of a solid sample (see Fig. 3 and Table 2), with no evidence for the presence of other species. Thus the results of the ^{77}Se, ^{14}N NMR and Raman spectra are consistent with retention of the $SeNSeNSe^{2+}$ ring in solution, in contrast to $SNSNS^{2+}$ in $SNSNS(AsF_6)_2$[21,23] which completely dissociates in solution. The $SeNSNSe^{2+}$ cation (as the AsF_6^- salt) also retains its ring structure in solution.[10]

We envisaged that if the $SeNSeNSe^{2+}$ cation dissociates in solution, then $F_3CC{\equiv}CCF_3$ or $SNAsF_6$ might react with $SeNSe^+$ to give $F_3CCSeNSeCCF_3^+$ and $SeNSNSe(AsF_6)_2$, respectively (*cf.* quantitative concerted symmetry-allowed reactions of SNS^+ with $F_3CC{\equiv}CCF_3$[36] and NS^+[21-23]). However, there was no evidence (^{77}Se, ^{14}N NMR, IR spectra, no weight increase) for these reactions occurring. It is possible that the planar dication may be in a rapid equilibrium with very small amounts of **II** on the NMR time-scale, thus rendering all selenium atoms equivalent. Thus $SeNSeNSe^{2+}$ may be rendered fluxional by an intramolecular* process reminiscent of the fluxional structures of several organic[37] and inorganic[38] compounds.

The X-Ray Crystal Structures of $(SeNSeNSe)_n(AsF_6)_2$ (*n* = 1 *or* 2).—The X-ray crystal structure of $SeNSeNSe(AsF_6)_2$ consists of discrete, planar $SeNSeNSe^{2+}$ cations and distorted AsF_6^- ions with strong interionic interactions. The $SeNSeNSe^{2+}$ cation is shown in Fig. 6 which also includes estimated† π-bond orders and average bond distances in $SeNSeNSe^{2+}$, $SeNSeNSe^{\bullet+}$, $SeNSNSe^{2+}$ and $SeNSNSe^{\bullet+}$. The bond distances and angles within the $SeNSeNSe^{2+}$ cation and anions are listed in Table 5. The structures of $SeNSeNSe(AsF_6)_2$, $SeNSNSe(AsF_6)_2$[10] and $SNSNS(AsF_6)_2$[21,23] are all isomorphous (space group *C*2) and isostructural.

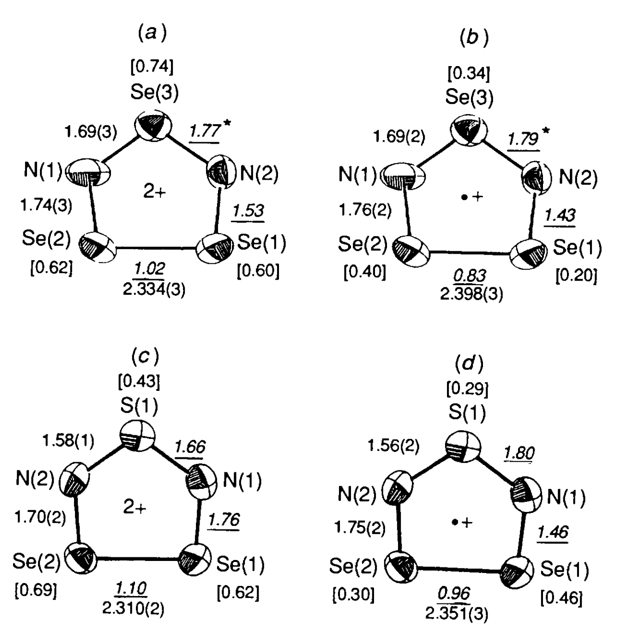

Fig. 6 An ORTEP plot of the $SeNSeNSe^{2+}$ cation and calculated bond orders† (ref. 39) (underlined and in italics), average bond lengths (Å) and sum of bond valences of the Se···F and S···F contacts (ref. 40) (in square brackets) in $SeNSeNSe^{2+}$ (*a*), $SeNSeNSe^{\bullet+}$ (*b*), $SeNSNSe^{2+}$ (*c*) and $SeNSNSe^{\bullet+}$ (*d*). Asterisk indicates calculated using 1.690(20) and 1.694(27) Å for the monocation and dication, respectively)

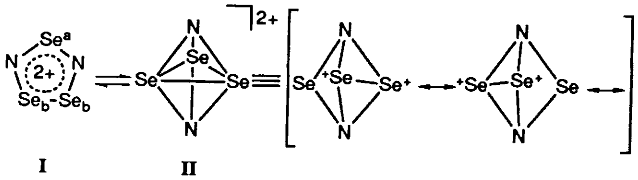

I II

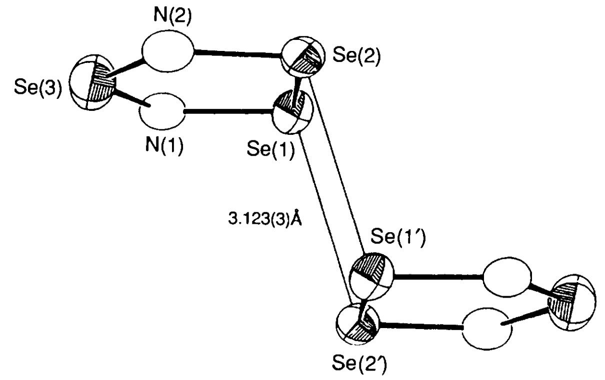

Fig. 7 An ORTEP plot of the $(SeNSeNSe^{\bullet+})_2$ cation. The numbering of atoms in the other independent dimer are given in Fig. 9(*b*)

The X-ray crystal structure of $(SeNSeNSe)_2(AsF_6)_2$ consists of two identical, but crystallographically different, discrete dimeric $(SeNSeNSe^{\bullet+})_2$ cations and distorted AsF_6^- anions with significant interionic interactions. The bond distances and angles within the two dimeric cations are essentially the same. These are listed in Table 6 which also includes bond distances and angles within the anions. Each $(SeNSeNSe^{\bullet+})_2$ cation consists of two planar $SeNSeNSe^{\bullet+}$ monomers weakly linked into a *trans* centrosymmetric geometry by two long Se···Se contacts [2 × 3.123(3), 2 × 3.149(3) Å] as shown in Fig. 7. The $SeNSeNSe^{\bullet+}$ radical cations dimerise by overlap of their selenium-based π* SOMO as observed in related compounds (see below). The overall *trans* geometry of $(SeNSeNSe^{\bullet+})_2$ is similar to those in $(SeNSNSe^{\bullet+})_2(AsF_6^-)_2$.[30] [Se···Se 3.159(2), 3.111(2) Å], $(Se/SNSNSe^{\bullet+})_2(AsF_6^-)_2$[24] [Se/S···Se

---

* It is possible that further cooling could result in the observation of different chemical shifts corresponding to Se_A and Se_B with appropriate satellite peaks due to ^{77}Se–^{77}Se coupling.

† The bond order (*N*) was calculated by the Pauling equation $N = 10^{(D-R)/0.71}$, where *R* is the observed bond length (Å) and *D* the sum of the appropriate covalent radii (Å) for a single bond; *D* = 2.34 and 1.87 Å for Se–Se and Se–N respectively (ref. 39) and 2.04 Å for S–S (ref. 41).

Table 5 Bond distances (Å) and angles (°) for $\mathrm{SeNSeNSe(AsF_6)_2}$ with e.s.d.s in parentheses *

$\mathrm{SeNSeNSe}^{2+}$			
Se(1)–Se(2)	2.334(3)	Se(1)–N(2)–Se(3)	122(1)
Se(1)–N(2)	1.73(1)	N(2)–Se(3)–N(1)	103.8(9)
Se(3)–N(2)	1.70(1)	Se(3)–N(1)–Se(2)	123(1)
Se(3)–N(1)	1.69(2)	N(1)–Se(2)–Se(1)	95.2(5)
Se(2)–N(1)	1.74(2)	Se(2)–Se(1)–N(2)	95.8(7)
$\mathrm{AsF_6}^-$			
As(1)–F(11)	1.63(2)	As(3)–F(31)	1.76(2)
As(1)–F(12)	1.68(2)	As(3)–F(32)	1.66(1)
As(1)–F(13)	1.66(2)	As(3)–F(33)	1.76(2)
As(2)–F(21)	1.68(2)	As(3)–F(34)	1.72(2)
As(2)–F(22)	1.78(2)	As(3)–F(35)	1.64(1)
As(2)–F(23)	1.66(2)	As(3)–F(36)	1.62(1)
F(11)–As(1)–F(11b)	96(1)	F(11b)–As(1)–F(12b)	176(1)
F(11)–As(1)–F(12)	176(1)	F(11b)–As(1)–F(13)	93(2)
F(11)–As(1)–F(12b)	88(1)	F(11b)–As(1)–F(13b)	96(1)
F(11)–As(1)–F(13)	96(1)	F(12b)–As(1)–F(13)	85(1)
F(11)–As(1)–F(13b)	93(2)	F(12b)–As(1)–F(13b)	86(1)
F(11b)–As(1)–F(12)	88(1)	F(13)–As(1)–F(13b)	167(2)
F(21)–As(2)–F(21f)	174(2)	F(23)–As(2)–F(23f)	90.6(9)
F(21)–As(2)–F(22)	88(1)	F(21f)–As(2)–F(22)	87(1)
F(21)–As(2)–F(22f)	87(1)	F(21f)–As(2)–F(22f)	88(1)
F(21)–As(2)–F(23)	89(1)	F(21f)–As(2)–F(23)	95(1)
F(21)–As(2)–F(23f)	95(1)	F(21f)–As(2)–F(23f)	89(1)
F(22)–As(2)–F(23f)	92.4(9)	F(22)–As(2)–F(22f)	84.6(9)
F(22f)–As(2)–F(23)	92.4(9)	F(22)–As(2)–F(23)	176.3(9)
F(22f)–As(2)–F(23f)	176.3(9)		
F(31)–As(3)–F(32)	175(1)	F(32)–As(3)–F(36)	94.7(9)
F(31)–As(3)–F(33)	87(1)	F(33)–As(3)–F(34)	88(1)
F(31)–As(3)–F(34)	87(1)	F(33)–As(3)–F(35)	176(1)
F(31)–As(3)–F(35)	89.6(9)	F(33)–As(3)–F(36)	88(1)
F(31)–As(3)–F(36)	90(1)	F(34)–As(3)–F(35)	90(1)
F(32)–As(3)–F(33)	91.7(8)	F(34)–As(3)–F(36)	174(1)
F(32)–As(3)–F(34)	89(1)	F(35)–As(3)–F(36)	95.0(9)
F(32)–As(3)–F(35)	91.6(7)		

* The lower case letters appended to the atom numbers refer to various symmetry-equivalent positions of the given atom.

Table 6 Bond distances (Å) and angles (°) in the two independent $\mathrm{(SeNSeNSe)_2(AsF_6)_2}$ dimers with e.s.d.s in parentheses (see footnote to Table 5)

$(\mathrm{SeNSeNSe}^{\bullet+})_2$ in dimer 1			
Se(1)–Se(2)	2.398(3)	Se(1)–N(1)–Se(3)	120.8(8)
Se(1)–N(1)	1.76(2)	Se(2)–N(2)–Se(3)	120.6(8)
Se(3)–N(1)	1.69(2)	Se(1)–Se(2)–N(2)	95.6(5)
Se(3)–N(2)	1.69(1)	Se(2)–Se(1)–N(1)	95.2(5)
		N(1)–Se(3)–N(2)	107.7(7)
Se(2)–N(2)	1.76(1)	N(1)–Se(1)–Se(2′)	106.6(5)
Se(1) ··· Se(2′)	3.123(3)	N(2)–Se(2)–Se(1′)	107.7(5)
		Se(1)–Se(2)–Se(1′)	89.31(8)
		Se(2)–Se(1)–Se(2′)	90.69(8)
$(\mathrm{SeNSeNSe}^{\bullet+})_2$ in dimer 2			
Se(4)–Se(5)	2.395(3)	Se(4)–N(3)–Se(6)	120.9(8)
Se(4)–N(3)	1.74(1)	Se(5)–N(4)–Se(6)	120.8(8)
Se(6)–N(3)	1.72(1)	Se(4)–Se(5)–N(4)	95.5(4)
Se(6)–N(4)	1.70(1)	Se(5)–Se(4)–N(3)	96.1(4)
Se(5)–N(4)	1.77(1)	N(3)–Se(6)–N(4)	106.7(7)
Se(4) ··· Se(5′)	3.149(3)	N(3)–Se(4)–Se(5′)	105.1(5)
		N(4)–Se(5)–Se(4′)	105.6(5)
		Se(4)–Se(5)–Se(4′)	89.13(8)
		Se(5)–Se(4)–Se(5′)	90.87(8)
$\mathrm{AsF_6}^-$			
As(1)–F(11)	1.65(1)	As(2)–F(21)	1.70(1)
As(1)–F(12)	1.73(1)	As(2)–F(22)	1.71(1)
As(1)–F(13)	1.68(1)	As(2)–F(23)	1.61(2)
As(1)–F(14)	1.69(1)	As(2)–F(24)	1.67(2)
As(1)–F(15)	1.64(1)	As(2)–F(25)	1.63(2)
As(1)–F(16)	1.68(1)	As(2)–F(26)	1.67(1)
F(11)–As(1)–F(12)	87.8(7)	F(12)–As(1)–F(16)	89.8(7)
F(11)–As(1)–F(13)	176.9(9)	F(13)–As(1)–F(14)	89.0(7)
F(11)–As(1)–F(14)	92.1(7)	F(13)–As(1)–F(15)	88.2(8)
F(11)–As(1)–F(15)	94.7(9)	F(13)–As(1)–F(16)	88.6(9)
F(11)–As(1)–F(16)	89(1)	F(14)–As(1)–F(15)	93.5(9)
F(12)–As(1)–F(13)	90.8(6)	F(14)–As(1)–F(16)	85.9(9)
F(12)–As(1)–F(14)	175.7(8)	F(15)–As(1)–F(16)	176.7(9)
F(12)–As(1)–F(15)	90.8(4)		
F(22)–As(2)–F(24)	90.0(8)	F(22)–As(2)–F(26)	89.7(7)
F(22)–As(2)–F(25)	90.8(8)	F(23)–As(2)–F(24)	178(1)
F(21)–As(2)–F(22)	178.0(8)	F(23)–As(2)–F(25)	98(1)
F(21)–As(2)–F(23)	91.1(8)	F(23)–As(2)–F(26)	86(1)
F(21)–As(2)–F(24)	88.4(8)	F(24)–As(2)–F(25)	84(1)
F(21)–As(2)–F(25)	90.2(9)	F(24)–As(2)–F(26)	92(1)
F(21)–As(2)–F(26)	89.1(8)	F(25)–As(2)–F(26)	176(1)
F(22)–As(2)–F(23)	90.4(8)		

3.077(3), 3.138(3) Å] and $(\mathrm{SNSNS}^{\bullet+})_2(\mathrm{X}^-)_2$ [S···S, X = $\mathrm{S_2O_6Cl}$, 3.027;[42a] $\mathrm{AsF_6}$, 2.994(3); $\mathrm{CF_3SO_3}$, 2.996(2); $\mathrm{S_2O_2F}$, 2.986(1); $\mathrm{SO_3F}$, 3.030(1) Å].[42b]

The Se(1)–Se(2) bond in $\mathrm{SeNSeNSe}^{2+}$ is significantly shorter (*i.e.* more than 3σ) than that in $\mathrm{SeNSeNSe}^{\bullet+}$; the Se(2)–N(1) bond in the dication is shorter than the corresponding bond in the monocation, although the difference is not significant, whereas the Se(3)–N(1) bonds are essentially the same in the two cations (see Fig. 6). The changes in the bond distances which accompany the oxidation of $\mathrm{SeNSeNSe}^{\bullet+}$ to $\mathrm{SeNSeNSe}^{2+}$ are therefore consistent with the nature of the SOMO of $\mathrm{SeNSeNSe}^{\bullet+}$ (assuming it is the same as that of $\mathrm{SNSNS}^{\bullet+}$,[31,42,43] see **III** which is unoccupied in the dication). The antibonding interactions between Se(1)–Se(2) and Se(2)–N(1) cause the bonds to shorten on removal of the single electron whereas there is little effect on S(3)–N(1) because of the node through Se(3).

The species $\mathrm{SeNSeNSe}^{2+}$ and $(\mathrm{SeNSeNSe})_2{}^{\bullet+}$ are formally 6π and 7π systems, respectively. The π-bond orders estimated from the bond distances indicate the presence of thermodynamically stable delocalised $4\mathrm{p}_\pi(\mathrm{Se})$–$2\mathrm{p}_\pi(\mathrm{N})$ bonds consistent with a simple MO model derived from that of SNSNS^{2+}.[21,23] However, the calculated Se–Se bond orders in $\mathrm{SeNSeNSe}^{2+}$ (1.02) and $(\mathrm{SeNSeNSe})_2{}^{\bullet+}$ (0.83) are very much lower than expected on the basis of the MO treatment which indicates a substantial $4\mathrm{p}_\pi$–$4\mathrm{p}_\pi$ contribution from the totally symmetric bonding MO in the Se–Se region. Long Se–Se bonds are also observed in $\mathrm{SeNSNSe}^{2+}$ (bond order 1.10) and $(\mathrm{SeNSNSe})_2{}^{\bullet+}$ (0.96), although they are significantly shorter than those in $\mathrm{SeNSeNSe}^{n+}$ (n = 1 or 2, see Fig. 6). Similar and even more pronounced weakening effects are present in $(\mathrm{SNSNS}^{\bullet+})_2$ [S–S 2.147(3) Å, bond order 0.71][42] and SNSNS^{2+} [S–S 2.093(5) Å, 0.84][23] in which the S–S bonds are 0.107 and 0.053 Å respectively longer than the normal S–S single bond (2.04 Å)[41] whereas there is significant π bonding within the S–N bonds. The long chalcogen–chalcogen bond may result in part from some lengthening of the bond due to repulsion of the two adjacent positively charged chalcogen atoms as illustrated by

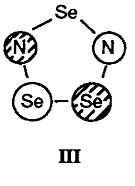

III

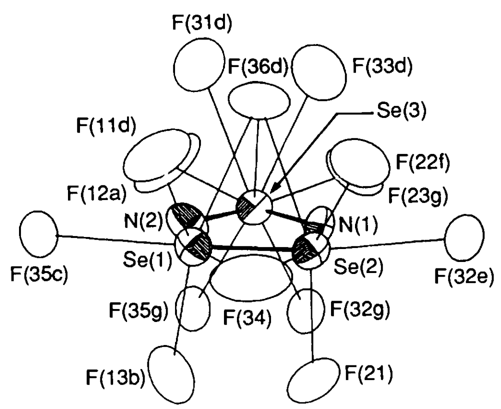

Fig. 8 Cation–anion contacts in $\overline{SeNSeNSe}(AsF_6)_2$

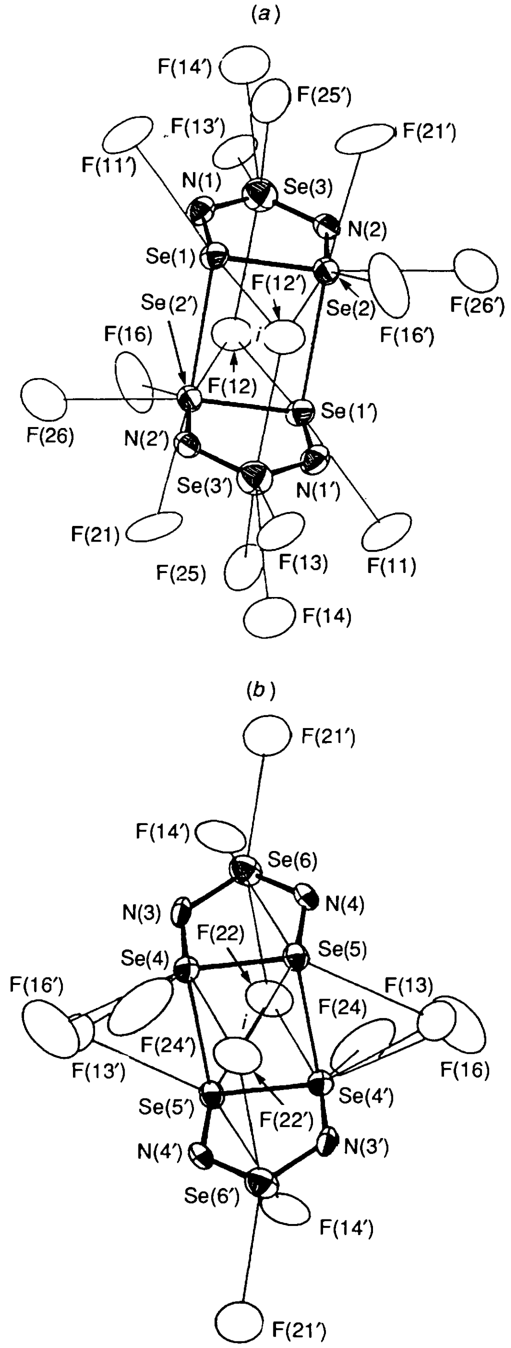

Fig. 9 Cation–anion contacts in $(\overline{SeNSeNSe})_2(AsF_6)_2$: (*a*) dimer 1; (*b*) dimer 2. The primed and unprimed atom labels refer to symmetry-equivalent atoms related by a crystallographic inversion centre at ½, ½, 0 (dimer 1) and ½, 0, ½ (dimer 2)

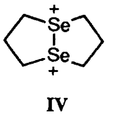

IV

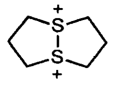

V

the long Se^+–Se^+ [2.382(2) Å, bond order 0.86] and S^+–S^+ bonds (2.124 Å, 0.76) in $C_6H_{12}Se_2(S_2)^{2+}$ **IV** and **V**, respectively.[44]

Cation–Anion Interactions in $(\overline{SeNSeNSe})_n(AsF_6)_2$ (*n* = 1 *or* 2).—There are significant interionic interactions between the fluorine atoms of the AsF_6^- anions and the $\overline{SeNSeNSe}^{2+}$ and $(\overline{SeNSeNSe}^{\bullet+})_2$ cations as shown in Figs. 8 and 9. The corresponding cation–anion contacts that are less than the sum of the isotropic van der Waals radii for Se ··· F 3.37 Å[45] are listed in Tables 7 and 8 for $\overline{SeNSeNSe}^{2+}$ and $(\overline{SeNSeNSe}^{\bullet+})_2$, respectively. The number of significant Se ··· F contacts in $\overline{SeNSeNSe}^{2+}$ is essentially the same as those in $(\overline{SeNSeNSe}^{\bullet+})_2$ but they are shorter in the dication than in the monocation, consistent with the dipositive charge in the former. This is illustrated by the sum of bond valences* for the Se ··· F contacts which is considerably higher in $\overline{SeNSeNSe}^{2+}$ than in $(\overline{SeNSeNSe}^{\bullet+})_2$ (see Fig. 6). The chalcogen–nitrogen bond orders seem to correlate with the sum of bond valences and thus positive charge on the chalcogen; the higher the charge the greater is the donation of electrons from nitrogen. Thus the Se(3)–N(2) bond order is 1.77 and N(2)–Se(1) is 1.53 in $\overline{SeNSeNSe}^{2+}$ reflecting the higher charge on Se(3). Conversely, the charge is higher on Se(1) and Se(2) in $\overline{SeNSNSe}^{2+}$ than in $\overline{SeNSeNSe}^{2+}$ and consistently the Se(1)–N(1) bond order (1.76) is higher than that of S(1)–N(1) (1.66) (see Fig. 6). There are no N ··· F contacts in both $\overline{SeNSeNSe}^{2+}$ and $(\overline{SeNSeNSe}^{\bullet+})_2$ implying zero or negative charge on the nitrogen atoms consistent with the weakness of nitrogen–fluorine bonding and the calculated charge on N (−0.45) in $\overline{SNSNS}(AsF_6)_2$.[21,23] The distribution of the positive charge in $\overline{SeNSeNSe}^{2+}$ is similar to that in $\overline{SNSNS}^{2+}$ for which 6-31G* calculation placed the positive charge on the sulfur atoms [S(3), +1.2; S(1), S(2), +0.86] consistent with the sums of the S ··· F contact valences [S(3), 0.62; S(1), S(2) 0.5 bond valence units].

The pattern of cation–anion contacts in $\overline{SeNSeNSe}^{2+}$ is essentially identical to those observed in the isostructural analogues $\overline{SeNSNSe}^{2+}$ [10] and $\overline{SNSNS}^{2+}$ [21,23] and that in $(\overline{SeNSeNSe}^{\bullet+})_2$ is very similar to those in $(\overline{SeNSNSe}^{\bullet+})_2$[30] and various salts of $(\overline{SNSNS}^{\bullet+})_2$.[42] The pattern of these interionic contacts has been discussed in detail elsewhere.[10,21,30,42]

Conclusions

We have successfully prepared $(\overline{SeNSeNSe})_n(AsF_6)_2$† (*n* = 1 and 2) and characterised these salts in solution and in the solid state.

---

* The relative magnitudes of the bond valences[40] can be used to assess the strength of the Se ··· F contacts. Bond valence (BV) in valence units is given by $BV = (R/R_o)^{-n}$, where *R* is the observed bond distance (Å), $R_o = 1.17$, $n = 4.0$ for Se^{IV}–F. The actual formal oxidation state of the Se is in fact not IV but between II and IV.

† Interestingly we have found that freshly prepared 'Se_4N_2'[4a] when treated with AsF_5 in a ratio 1 : 3 in SO_2 at low temperature, led to the formation of $Se_3N_2(AsF_6)_2$ and $Se_4(AsF_6)_2$, as well as traces of $(Se_3N_2)_2(AsF_6)_2$ and $Se_8(AsF_6)_2$ (IR, FT-Raman, ^{77}Se NMR).[46] Ratios of 'Se_4N_2' and AsF_5 of 1 : 1.35 gave only $Se_4(AsF_6)_2$ in line with the results reported in ref. 47.

Table 7 Interionic contacts* (Å) and selected angles (°) for $SeNSeNSe^{2+}$ with e.s.d.s in parentheses

Se(1) ··· F(12a)	2.75(2)	Se(2) ··· F(21e)	2.95(2)
Se(1) ··· F(13b)	2.99(2)	Se(2) ··· F(22f)	2.71(2)
Se(1) ··· F(34)	2.71(2)	Se(2) ··· F(32e)	3.06(1)
Se(1) ··· F(35c)	3.08(1)	Se(2) ··· F(34)	2.68(2)
Se(1) ··· F(36d)	3.25(1)	Se(2) ··· F(36d)	3.22(1)
F(12a)–Se(1)–F(13b)	149.4(7)	F(21e)–Se(2)–F(22f)	149.8(6)
F(13b)–Se(1)–F(34)	105.1(8)	F(21e)–Se(2)–F(32e)	92.3(5)
F(13b)–Se(1)–F(35c)	84.8(5)	F(21e)–Se(2)–F(34)	101.5(7)
F(13b)–Se(1)–F(36d)	147.1(7)	F(21e)–Se(2)–F(36d)	146.9(6)
F(34)–Se(1)–F(35c)	117.5(6)	F(32e)–Se(2)–F(36d)	103.7(4)
F(34)–Se(1)–F(36d)	94.9(5)	F(34)–Se(2)–F(36d)	96.1(5)
F(35c)–Se(1)–F(36d)	108.9(4)		
Se(3) ··· F(11d)	2.74(2)	Se(3) ··· F(33d)	3.14(2)
Se(3) ··· F(23g)	2.80(2)	Se(3) ··· F(35g)	3.06(1)
Se(3) ··· F(31d)	3.22(2)	Se(3) ··· F(36d)	3.25(2)
Se(3) ··· F(32g)	3.02(1)		
(3)–F(23g)	89.8(7)	F(23g)–Se(3)–F(36d)	104.1(5)
F(11d)–Se(3)–F(32g)	96.3(5)	F(31d)–Se(3)–F(32g)	153.3(6)
F(11d)–Se(3)–F(33d)	94.0(7)	F(32g)–Se(3)–F(36d)	155.4(4)
F(11d)–Se(3)–F(36d)	106.2(5)	F(33d)–Se(3)–F(35g)	153.7(5)
F(23g)–Se(3)–F(31d)	95.7(6)	F(35g)–Se(3)–F(36d)	155.4(4)
F(23g)–Se(3)–F(35g)	99.1(4)		
Se(1)–Se(2)–F(21e)	92.9(4)	Se(2)–Se(1)–F(12a)	105.0(5)
Se(1)–Se(2)–F(22f)	108.7(4)	Se(2)–Se(1)–F(13b)	97.4(4)
Se(1)–Se(2)–F(32e)	172.9(3)	Se(2)–Se(1)–F(34)	63.6(5)
Se(1)–Se(2)–F(34)	65.0(5)	Se(2)–Se(1)–F(35c)	177.2(3)
Se(1)–Se(2)–F(36d)	69.4(3)	Se(2)–Se(1)–F(36d)	68.3(3)
N(2)–Se(1)–F(12a)	118.8(8)	N(1)–Se(2)–F(21e)	82.0(8)
N(2)–Se(1)–F(13b)	78.5(9)	N(1)–Se(2)–F(22f)	115.4(7)
N(2)–Se(1)–F(34)	159.3(8)	N(1)–Se(2)–F(32e)	80.8(7)
N(2)–Se(1)–F(35c)	82.9(8)	N(1)–Se(2)–F(34)	159.9(7)
N(2)–Se(1)–F(36d)	73.9(7)	N(1)–Se(2)–F(36d)	72.3(6)
N(1)–Se(3)–F(11d)	169.8(8)	N(2)–Se(3)–F(11d)	85.0(9)
N(1)–Se(3)–F(23g)	81.1(7)	N(2)–Se(3)–F(23g)	173.8(8)
N(1)–Se(3)–F(31d)	112.8(7)	N(2)–Se(3)–F(31d)	78.9(8)
N(1)–Se(3)–F(32g)	84.1(7)	N(2)–Se(3)–F(32g)	118.4(7)
N(1)–Se(3)–F(33d)	77.8(7)	N(2)–Se(3)–F(33d)	114.1(8)
N(1)–Se(3)–F(35g)	120.2(6)	N(2)–Se(3)–F(35g)	81.8(7)
N(1)–Se(3)–F(36d)	72.0(7)	N(2)–Se(3)–F(36d)	74.2(8)

* Includes all contacts less than the sum of the isotropic van der Waals radius for Se ··· F 3.37 Å, ref. 45. See footnote to Table 5.

These compounds contain the first fully characterised thermally stable binary Se–N species and are potentially useful precursors to a wide variety of new selenium–nitrogen compounds. The preparation of these compounds from the reactions of Se_4N_4 with stoichiometric quantities of AsF_5 is accompanied by loss of N_2 and illustrates one difference between Se_4N_4 and S_4N_4 chemistry. The isolation of the $SeNSeNSe^{\cdot+}$ radical cation on a preparative scale enabled us to obtain its ESR spectrum in SO_2 solution and as a frozen powder to show that the previous assignment[7] of the ESR spectrum obtained from powdered $SeNSNSe(AsF_6)_2$ in frozen D_2SO_4 or SO_2 to a mixture of $SeNSNSe^{\cdot+}$ and $SeNSeNSe^{\cdot+}$ was erroneous. The ^{77}Se NMR chemical shift (δ 2434) of $SeNSeNSe^{2+}$ is the highest so far reported and is consistent with its dipositive charge and 'electron-rich' aromatic 6π character. However, one rather than the expected two resonances for $SeNSeNSe^{2+}$ was observed in the ^{77}Se NMR spectrum consistent with fluxional behaviour which renders all selenium atoms equivalent on the NMR time-scale. Nevertheless $SeNSeNSe^{2+}$ like the related $SeNSNSe^{2+}$ [10] and $SeNSNS^{2+}$ [24] retains its ring structure in solution in contrast to $SNSNS^{2+}$ in $SNSNS(AsF_6)_2$ [21,23] which dissociates to SNS^+ and SN^+. This is consistent with the greater tendency of selenium-(IV) and -(VI) compounds to form polymeric (σ bonded) species relative to sulfur analogues (*e.g.* SeO_2 is polymeric whereas SO_2 is monomeric).[38]

Table 8 Interionic contacts* (Å) and selected angles (°) for the two independent $(SeNSeNSe^{\cdot+})_2$ cations with e.s.d.s in parentheses

Dimer 1			
Se(1) ··· F(11′)	3.16(1)	F(11′)–Se(1)–F(12′)	124.9(4)
Se(1) ··· F(12′)	2.94(1)		
Se(2) ··· F(12′)	2.88(1)	F(12′)–Se(2)–F(21′)	94.9(4)
Se(2) ··· F(16′)	3.07(2)	F(12′)–Se(2)–F(26′)	112.0(5)
Se(2) ··· F(21′)	3.20(1)	F(16′)–Se(2)–F(21′)	63.7(4)
Se(2) ··· F(26′)	3.04(2)	F(16′)–Se(2)–F(26′)	70.7(5)
		F(21′)–Se(2)–F(26′)	77.8(4)
Se(3) ··· F(12)	3.04(1)	F(12)–Se(3)–F(13′)	94.5(3)
Se(3) ··· F(13′)	3.22(2)	F(12)–Se(3)–F(14′)	136.9(3)
Se(3) ··· F(14′)	3.20(2)		
Se(3) ··· F(25′)	3.22(2)		
Dimer 2			
Se(4) ··· F(13′)	3.33(2)	F(16′)–Se(4)–F(22′)	90.2(4)
Se(4) ··· F(16′)	3.18(2)	F(16′)–Se(4)–F(24′)	59.9(5)
Se(4) ··· F(22′)	2.93(1)		
Se(4) ··· F(24′)	3.04(2)	F(13′)–Se(5)–F(14′)	134.6(4)
Se(5) ··· F(13′)	3.22(1)	F(13′)–Se(5)–F(22′)	92.5(4)
Se(5) ··· F(14′)	3.32(1)	F(14′)–Se(5)–F(22′)	94.6(3)
Se(5) ··· F(22′)	2.92(1)	F(21′)–Se(6)–F(22)	135.6(3)
Se(6) ··· F(21′)	3.02(1)		
Se(6) ··· F(22)	3.14(1)		

* Includes all contacts less than the sum of the isotropic van der Waals radii for Se ··· F 3.37 Å, ref. 45. Equivalent selenium atoms (related by a centre of inversion) in the dimer have the same number of fluorine contacts.

Acknowledgements

We thank the Natural Sciences and Engineering Research Council (Canada) for financial support and Dr. W. V. F. Brooks for the results of normal coordinate analyses of $SeNSeNSe(AsF_6)_2$ and related compounds and Janice L. Howe (Bruker, Canada) for the FT-Raman spectra of $Se_3N_2(AsF_6)_2$. We are also indebted to Dr. J. A. Hugh MacBride of University of Durham for suggesting that $SeNSeNSe^{2+}$ may be fluxional in solution thus rendering all the selenium atoms equivalent in the ^{77}Se NMR spectrum.

References

1 (*a*) H. G. Heal, *The Inorganic Heterocyclic Chemistry of Sulfur, Nitrogen, and Phosphorus*, Academic Press, London, 1980; T. Chivers and R. T. Oakley, *Top. Curr. Chem.*, 1982, **102**, 117; T. Chivers, *Acc. Chem. Res.*, 1984, **17**, 166; R. Gleiter, *Angew. Chem., Int. Ed. Eng.*, 1981, **20**, 444; (*b*) R. T. Oakley, *Prog. Inorg. Chem.*, 1988, **36**, 299; (*c*) J. P. Johnson, J. Passmore, P. S. White, A. J. Banister and A. G. Kendrick, *Acta Crystallogr., Sect. C*, 1987, **43**, 1651.

2 Y. K. Kudo and S. Hamanda, *Bull. Chem. Soc. Jpn.*, 1983, **56**, 2627.

3 C. K. Barker, A. W. Cordes and G. L. Margrave, *J. Phys. Chem.*, 1965, **69**, 334.

4 (*a*) K. Dehnicke, F. Schmock, K. F. Kohler and G. Frenking, *Angew. Chem., Int. Ed. Engl.*, 1991, **30**, 577; (*b*) J. Siivari, T. Chivers and R. S. Laitinen, 75th Canadian Chemical Conference, Edmonton, Alberta, June 1992; *Angew Chem., Int. Ed. Engl.*, in the press.

5 J. Passmore, G. Sutherland and P. S. White, *J. Chem. Soc., Chem. Commun.*, 1980, 330; M. P. Murchie, J. Passmore, G. W. Sutherland and R. Kapoor, *J. Chem. Soc., Dalton Trans.*, 1992, 503.

6 J. P. Johnson, G. K. MacLean, J. Passmore and P. S. White, *Can. J. Chem.*, 1989, **67**, 1687.

7 E. Awere, J. Passmore, K. F. Preston and L. H. Sutcliffe, *Can. J. Chem.*, 1988, **66**, 1776.

8 N. Burford, J. Passmore and M. J. Schriver, *J. Chem. Soc., Chem. Commun.*, 1986, 140; W. V. F. Brooks, N. Burford, J. Passmore, M. J. Schriver and L. H. Sutcliffe, *J. Chem. Soc., Chem. Commun.* 1987, 69; S. Mattar, J. Passmore and X. Sun, 75th Canadian Chemical Conference, Edmonton, Alberta, June 1992, Abstracts;

J. Passmore, X. Sun and S. Parsons, *Can. J. Chem.*, in the press; N. Burford, J. Passmore and X. Sun, unpublished work.

9 E. G. Awere, J. Passmore, P. S. White and T. Klapötke, *J. Chem. Soc., Chem. Commun.*, 1989, 1415.

10 E. G. Awere, J. Passmore and P. S. White, *J. Chem. Soc., Dalton Trans.*, 1992, 1267 and refs. therein.

11 E. G. Awere and J. Passmore, *J. Chem. Soc., Dalton Trans.*, 1992, 1343; J. Passmore and M. S. Schriver, *Inorg. Chem.*, 1988, **27**, 2749.

12 Brunnhilde v. Tschirschnitz-Geibler, *Gmelin Handbook of Inorganic Chemistry*, Se suppl. vol. B2, Springer, Berlin, 1984, p. 238 and refs. therein.

13 A. Apblett, A. J. Banister, D. Biron, A. G. Kendrick, J. Passmore, M. J. Schriver and M. Stojanac, *Inorg. Chem.*, 1986, **25**, 4451.

14 S. J. Kuhn, *Can. J. Chem.*, 1967, **45**, 3207 and refs. therein.

15 J. Jander and V. Doetsch, *Chem. Ber.*, 1960, **93**, 561.

16 D. M. Yost and J. B. Hatcher, *J. Am. Chem. Soc.*, 1983, **53**, 2549.

17 M. A. Armour, L. M. Browne and G. L. Weir, *Hazardous Chemicals Information and Disposal Guide*, Department of Chemistry, Alberta University, Edmonton, 1982, p. 181.

18 J. Adel, C. Ergezinger, R. Figge and K. Dehnicke, *Z. Naturforsch., Teil B*, 1988, **43**, 639.

19 G. Wolmerhauser, C. R. Brulet and G. B. Street, *Inorg. Chem.*, 1978, **17**, 3586.

20 H. Garcia-Fernandez, *Bull. Soc. Chim. Fr.*, 1973, 1210.

21 W. F. V. Brooks, T. S. Cameron, F. Grein, S. Parsons, J. Passmore and M. J. Schriver, *Inorg. Chem.*, submitted.

22 R. C. Burns, M. J. Collins, R. J. Gillespie and G. B. Schrobilgen, *Inorg. Chem.*, 1986, **25**, 4465.

23 W. V. F. Brooks, T. S. Cameron, F. Grein, S. Parsons, J. Passmore and M. J. Schriver, *J. Chem. Soc., Chem. Commun.*, 1991, 1079.

24 E. G. Awere, T. S. Cameron, J. Passmore and X. Sun, *J. Chem. Soc., Dalton Trans.*, submitted.

25 E. G. Awere, Ph.D. Thesis. University of New Brunswick, Fredericton, 1992.

26 Y. Le Page, P. S. White and E. J. Gabe, NRCCAD, An Enhanced CAD-4 Control Program, Annual Meeting of American Crystallographic Association, Hamilton, Ontario, 1986.

27 N. Walker and D. Stuart, *Acta Crystallogr., Sect. A*, 1983, **39**, 158.

28 E. J. Gabe, Y. Le Page, J.-P. Charland, F. L. Lee and P. S. White, *J. Appl. Crystallogr.*, 1989, **22**, 384.

29 *International Tables for X-Ray Crystallography*, Kynoch Press, Birmingham, 1974, vol. 4.

30 R. J. Gillespie, J. P. Kent and J. F. Sawyer, *Inorg. Chem.*, 1981, **20**, 4053.

31 S. A. Fairhurst, K. F. Preston and L. H. Sutcliffe, *Can. J. Chem.*, 1984, **62**, 1124.

32 S. A. Fairhurst, K. M. Johnson, L. H. Sutcliffe, K. F. Preston, A. J. Banister, Z. V. Hauptman and J. Passmore, *J. Chem. Soc., Dalton Trans.*, 1986, 1465.

33 K. F. Preston and L. H. Sutcliffe, *Magn. Reson. Chem.*, 1991, **28**, 189.

34 R. J. Gillespie, J. P. Kent, J. F. Sawyer and J. D. Tyrer, *Inorg. Chem.*, 1981, **20**, 3799.

35 (*a*) H. Hartl, P. Huppmann, D. Lentz and K. Seppelt, *Inorg. Chem.*, 1983, **22**, 2183; 1984, **23**, 510; (*b*) Ya. G. Bol'on and E. S. Levchenko, *Zh. Org. Khim.*, 1967, **3**, 777; J. S. Thrasher and K. Seppelt, *Z. Anorg. Allg. Chem.*, 1983, **507**, 7; J. S. Thrasher, C. W. Bauknight, jun. and D. D. Desmarteau, *Inorg. Chem.*, 1985, **24**, 1598; (*c*) F. Fockenberg and A. Haas, *Z. Naturforsch., Teil B*, 1986, **41**, 413; (*d*) N. Ya. Derkach, T. V. Lyapina and E. S. Levchenko, *J. Org. Chem. USSR* (*Engl. Transl.*), 1981, **17**, 536.

36 E. G. Awere, N. Burford, C. Mailer, J. Passmore, M. J. Shriver, P. S. White, A. J. Banister, H. Oberhammer and L. H. Sutcliffe, *J. Chem. Soc., Chem. Commun.*, 1987, 66.

37 See, for example, J. March, *Advanced Organic Chemistry: Reactions, Mechanism and Structure*, 3rd edn., Wiley-Interscience, New York, 1985, p. 1025.

38 N. N. Greenwood and A. Earnshaw, *Chemistry of the Elements*, Pergamon, Oxford, 1984.

39 L. Pauling, *The Nature of the Chemical Bond*, 3rd edn., Cornell University Press, Ithaca, NY, 1960.

40 I. D. Brown, in *Structure and Bonding in Crystals*, eds. M. O'Keefe and A. Navrotsky, Academic Press, London, 1981, vol. 2, p. 1.

41 R. Steudel, *Angew. Chem., Int. Ed. Engl.*, 1975, **14**, 655.

42 (*a*) A. J. Banister, H. G. Clarke, I. Rayment and H. M. M. Shearer, *Inorg. Nucl. Chem. Lett.*, 1974, **10**, 647; (*b*) R. J. Gillespie, J. P. Kent and J. F. Sawyer, *Inorg. Chem.*, 1981, **20**, 3784.

43 R. G. Gleiter, R. Bartetzko and P. Hofmann, *Z. Naturforsch., Teil B*, 1980, **35**, 1166.

44 F. Iwasaki, M. Morimoto, M. Yasui, R. Akaishi, H. Fujihara and N. Furukawa, *Acta Crystallogr., Sect. C*, 1991, **47**, 1463.

45 S. C. Nyburg and C. H. Faerman, *Acta Crystallogr., Sect. B*, 1985, **41**, 274.

46 P. MacKenzie, J. Passmore and G. Schatte, unpublished work.

47 T. Klapötke, in *The Chemistry of Inorganic Ring Systems*, ed. R. Steudel, Elsevier, Amsterdam, 1992, p. 409.

Received 10*th June* 1992; *Paper* 2/03060H